# EXPLOITING SINGULAR CONFIGURATIONS FOR CONTROLLABLE, LOW-POWER, FRICTION ENHANCEMENT ON UNMANNED GROUND VEHICLES

A Thesis
Presented to
The Academic Faculty

By

Adam J. Foris

In Partial Fulfillment
of the Requirements for the Degree
Master of Science in the
George W. Woodruff School of Mechanical Engineering

Georgia Institute of Technology
May 2020

# EXPLOITING SINGULAR CONFIGURATIONS FOR CONTROLLABLE, LOW-POWER, FRICTION ENHANCEMENT ON UNMANNED GROUND VEHICLES

*Approved by:*

Dr. A. Mazumdar, Advisor
School of Mechanical Engineering
*Georgia Institute of Technology*

Dr. K.M. Lee
School of Mechanical Engineering
*Georgia Institute of Technology*

Dr. F. Hammond
School of Mechanical Engineering
*Georgia Institute of Technology*

Dr. A. Young
School of Mechanical Engineering
*Georgia Institute of Technology*

*Date Approved:* March 02, 2020

This work is dedicated to my daughter, Jaida. May you find your passion and eclipse my accomplishments in your own unique way.

## ACKNOWLEDGEMENTS

I want to thank my advisor Dr. Anirban Mazumdar for the opportunity to conduct research alongside him. His great aptitude, creativity, and verve for pushing the unknown was both essential and inspiring.

I also want to thank my parents for their unconditional support in my every endeavor. Their confidence bolstered my own through the ebb and flow of this work.

Finally, I want to thank my companion, Sennen Peña, for her ever-present encouragement and support. Her positivity and optimism have proven contagious.

-Adam Foris

## TABLE OF CONTENTS

## LIST OF TABLES

## LIST OF FIGURES

## SUMMARY

Despite recent advancements in autonomous mobility on paved roads, off-road environments continue to pose significant performance obstacles. Autonomous vehicles subjected to widely varying terrain is a particularly difficult challenge. In such environments, maneuvering performance often relies on human intuition and intervention to maximize or even maintain the vehicle's traction. For instance, removable systems like tire chains can be installed to address icy conditions encountered mid-mission. Most autonomous platforms, however, are not equipped to conduct such installations on-the-fly, and removable systems act instead as permanent installations on the wheel. This is problematic because periodic performance degradation is commonly experienced by static configurations operating on heterogeneous terrain. Adaptive solutions can help address the heterogeneous terrain problem by deploying traction-aiding devices but often require involved installations, are energy intensive, or are limited to a restrictive set of missions through the use of highly specific gripping elements or locomotion modes.

This work describes the design, validation, and performance of a new type of adaptive wheel morphology for unmanned ground vehicles. The adaptive wheel utilizes a novel, variable transmission-ratio spiral cam to enable controllable deployment of high-friction gripping elements. Expanded, the high-friction grippers make contact with the terrain and deliver component-level acceleration performance increases of 170% or more. Static friction testing of the gripper design suggests even greater potential, offering between 160% to 320% greater hold than the rubber tire. An important feature of this morphology is that if the grippers fail to outperform the wheel's original rubber tire on any particular surface, they can retract to allow uninhibited operation of the tire.

The mechanism's spiral cam exploits a singular configuration to minimize power consumption and protect the actuator from external forces. Through geometric manipulation of the spiral cam, a number of desired traits can be elicited, such as high gripper deployment

speed during expansion and retraction and low input actuator requirements. A mathematical basis for the spiral cam's design is developed in this work. Coupled with a low-footprint worm gear, the integrated drive train enables the use of small, inexpensive motors for mechanism actuation to reduce total system mass. The overall mechanism design is modular, self-powered via an integrated battery, and easily mounts to the existing wheels of a vehicle. The system controllably deploys, requires limited, low-power sensors, self-monitors battery charge, and utilizes a singular configuration in its deployed state.

Full-scale testing highlights both the feasibility of the traction-augmenting approach employed and the merit of the design. Compared to traditional static or quasi-static wheel technologies, this adaptive system offers dramatically improved traction on heterogeneous terrain. In terms of installation, the system is at least as easily installed as current technologies. The penalty incurred is its weight; even an optimized design is not expected to realistically approach the mass of systems like tire chains. In comparison to adaptive mechanisms, the primary advantages are its low-power consumption, modularity, customization, ease of installation on existing vehicles, and low impact on requisite vehicle modifications. Wheels need not be replaced by the system; they are modified by the system. The ability to readily install onto non-specific wheels produces an attractive use case for deployment on existing vehicles. Combined with ground property estimation and adaptive control, autonomous vehicle performance stands to increase considerably.

# CHAPTER 1
# INTRODUCTION AND BACKGROUND

## 1.1 Frictional Challenges on Varying Terrain

Achieving terrestrial mobility in diverse environments can transform how many important missions such as transportation, exploration, and monitoring are performed. While autonomous mobility on paved roads has seen major advancements, off-road and diverse terrain remain challenging. Varying conditions are particularly problematic for autonomous systems because they often lack the intuition, perception, and adaptive capacity of human drivers [1]. Human operators not only adapt their driving to modulate friction [2], they also physically modify their vehicles for different terrain. For instance, humans can influence the frictional performance of their vehicles by replacing the tires with off-road variants or adding chains ad hoc. This has proven effective [3], but autonomous systems cannot rely on a human expert to intervene every time the environment changes.

A feature of all traction devices is that performance is optimized for a particular terrain or set of terrains. When conditions are encountered outside of the performing set, friction can degrade appreciably [4]. For example, rubber tires grip dry pavement well but frictional performance suffers when the pavement is covered with snow or ice. In real time, the tire cannot be swapped for a more suitable configuration (i.e., a studded tire). Traditional quasi-static solutions like chains may be employed, but autonomous platforms cannot install them when needed. As a result, most quasi-static solutions on autonomous platforms bear more resemblance to a modified tire than a removable traction device. In light of the fact that off-road terrains tend to vary widely, a new approach is necessary to push traction performance boundaries across wider terrain sets.

This work presents a new type of adaptive wheel intended for friction modulation. The

core contributions of this work are the analysis, design, and validation of the spiral cam system that controllably deploys a set of terrain grippers. Deployed, the terrain grippers offer greatly improved traction on surfaces like ice. Retracted, the tire exclusively contacts the terrain. Controllable deployment thus expands the vehicle's working terrain-set by allowing independent use of special gripping elements or the original rubber tire. This unique, modular approach features easy attachment to existing vehicles and low power consumption through exploitation of a singular configuration. Additionally, this work demonstrates and quantifies the performance increase when this system is deployed on common off-road terrains.

## 1.2 Increasing Terrestrial Mobility

Terrestrial mobility, in this context, means maneuverability. Improving maneuverability requires that the gripping elements (i.e., *grippers*) of a vehicle remain kinetically static with respect to the terrain, ideally during any desired maneuver. The most common types of gripping elements vehicles employ off-road are wheels and tracks. When sufficient static friction exists for a given vehicle maneuver, the grippers remain in rolling contact with the terrain. Pure rolling minimizes frictional energy losses, allowing for greater vehicle range given the vehicle's energy storage capacity. Of equal importance is that static friction provides greater resistance to wheel forces than kinetic, or sliding, friction. Ensuring static, rolling contact maximizes the vehicle's hold on the terrain. On challenging terrains like ice, greater friction translates into better maneuverability.

Given their ubiquity to off-road environments, three surfaces are targeted in this work: ice, grass, and dry-packed dirt. Motivation for improving performance on such terrain also draws from experiments conducted with a 1:5 scale autonomous-vehicle, shown in Fig. 1.1. Extensive testing has demonstrated that aggressive vehicle maneuvering on dirt tracks is controllable in the presence of wheel slippage (i.e. during cornering) [5]. Aggressive maneuvering, as defined here, is vehicle maneuvering that exceeds the limits of handling

and is often associated with sudden collision avoidance or racing. Such maneuvering also notably induces gross wheel slippage in many instances. The basic idea underscoring this work is that if slip during aggressive maneuvers can be prevented, significant performance gains can be achieved. For the case of the Auto-Rally vehicle, which often aims to minimize racing times on a track, this translates into potentially significant reductions in racing times.

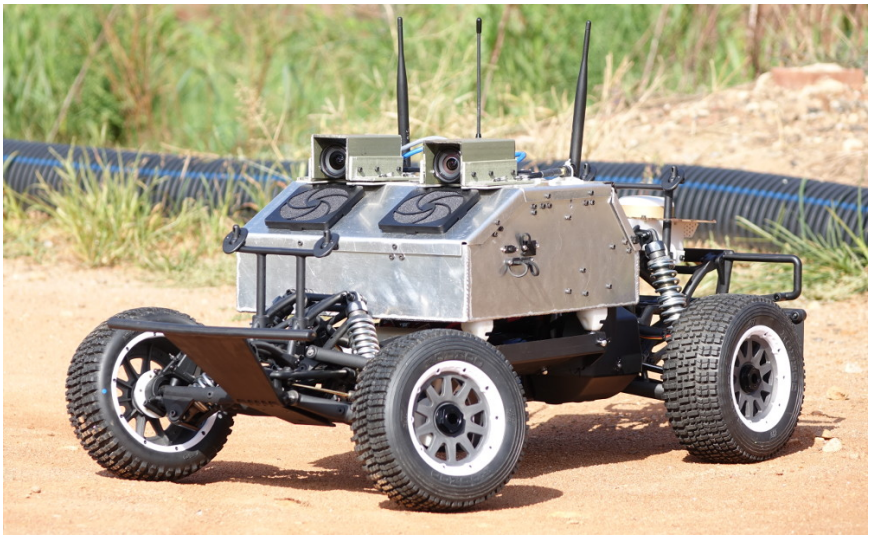

**Figure 1.1:** Wheeled, autonomous platforms like the Georgia Tech "Auto-Rally" vehicle [5] can greatly benefit from increases in traction, especially during aggressive maneuvering.

Two methods are available to improve vehicle maneuvering of similar autonomous platforms. One approach aims to enable aggressive driving through the use techniques like Model Predictive Control (MPC) [6] or combinations of MPC and Convolutional Neural Networks [7]. Such methods address control of the vehicle dynamics but do not modulate traction. A similar but distinctively different class of techniques have long been implemented in passenger vehicles to improve dynamic performance. Anti-lock brake (ABS) and generic traction control systems (TCS) monitor the relative rotation of a vehicle's wheels and modulate braking and/or drive-motor power to minimize wheel slip. The result is improved vehicle handling. For this latter class of techniques, emphasis is on minimizing wheel slip in adverse conditions. However, the inherent traction of the vehicle is not directly affected: the maximum available traction afforded by the vehicle's tire is limited by

the properties of the tire and its interaction with the terrain. Control techniques can better manage the vehicle's exploitation of the available traction but cannot improve it.

The second method of improving vehicle maneuvering aims to increase the maximum available traction. Techniques typically target the vehicle's gripping elements directly by incorporating features that indent the terrain. Categorically, most techniques are either static or quasi-static in nature. Static systems are permanently installed onto or into a wheel or tire, are not rapidly swapped for another system, and do not change configuration. Currently, a variety of static designs exist that are optimized for use on paved roads (i,e., ice or snow covered asphalt) [8]; for off-road environments, tires manufactured with accentuated features like deep pattern block grooves are common. Since static systems do not modulate behavior, they can be simple and robust to physical damage. Winter tires with embedded friction-enhancing studs are a good example of such static systems [9].

Quasi-static systems are readily installed on or removed from a wheel but once in place, mimic the behavior of a static system. The most commonly employed quasi-static system is the tire chain. Adverse conditions like snow or ice can be addressed, but the vehicle user must manually install the chains. This is advantageous because otherwise dry-pavement-optimized tires can be modified on-the-fly to address conditions problematic to the vehicle's tire. However, autonomous systems cannot deploy these systems in real time; a human operator is required for installation. The problem is that terrain is rarely homogeneous, and while the chain improves handling on an icy road, performance may suffer on temporary or prolonged stretches of dry pavement between icy patches.

The drawback of both static and quasi-static systems is thus that they cannot be easily changed and suffer from sub-optimal performance when used on terrain that differs from the design criteria [4]. As a result, there exists a growing research focus on adaptive ground locomotion systems that can adjust frictional properties dynamically. Existing adaptive methods fall into two broad categories: passive and active. Passive methods utilize mechanical intelligence to deploy or modify properties based on mechanical interaction be-

tween the vehicle and the terrain. These systems are desirable because they do not require power or communication. Incorporation of power or communication can add considerable complexity and failure modes to the system. Examples include spring-loaded variable diameter wheels [10, 11], wheels that can transform into legs [12], and footpads that deploy when slip occurs [13]. Similarly, spring-loaded microspines have shown great promise in this area and enable legged locomotion on vertical surfaces [14, 15]. Passive systems can be highly effective but cannot be easily modulated or controlled. As a result, they can be vulnerable to damage or wear when accidentally or improperly deployed.

Active systems require energy input to change configuration or sense the environment. Recent works have shown how wheel diameter can be modulated using flexible structures [16, 17] or linkages [18, 19]. Active systems can also provide the capacity to controllably transition between wheeled and legged locomotion [20, 21], wheeled and tracked motion [22, 23], or between legged, pseudo-wheeled, and tracked [24]. Besides altering the locomotion mode, wheels used as end-effectors on articulated arms feature the ability to change posture [25], allowing control of vehicle dynamics. A related system combines wheeled and legged locomotion and allows the wheel to transform between walking and rolling modes [26].

An inherent disadvantage is that active systems are generally difficult to deploy on wheels due to the rotation. Coupled with significant power requirements, active system often require complete replacement of the wheel. Active systems offer the most flexibility, but may be limited by their complexity, fragility, and power requirements. Energy efficiency is inherently reduced if the system requires actuator input to maintain posture. Furthermore, the system's actuator suite is commonly placed directly in the load path such that the propensity for gear or actuator failure heightens.

To be effective solutions for autonomous, off-road driving, active systems must dramatically modulate friction, draw little or no power, have minimal complexity, and be physically robust. They should also be easily integrated onto existing vehicles. In this

work, the proposed system can be fastened to an existing wheel via a simple mounting component, isolates the drive train from shocks experienced through the suspension, and consumes actuation power only when changing configuration. This design, highlighted in Fig. 1.2, utilizes a cam with a spiral profile that provides variable gearing and exploits a singular configuration when the mechanism is in a fully-expanded state. This system is self-powered and thereby obviates the use of slip-rings, can be controlled wirelessly, and minimizes power consumption.

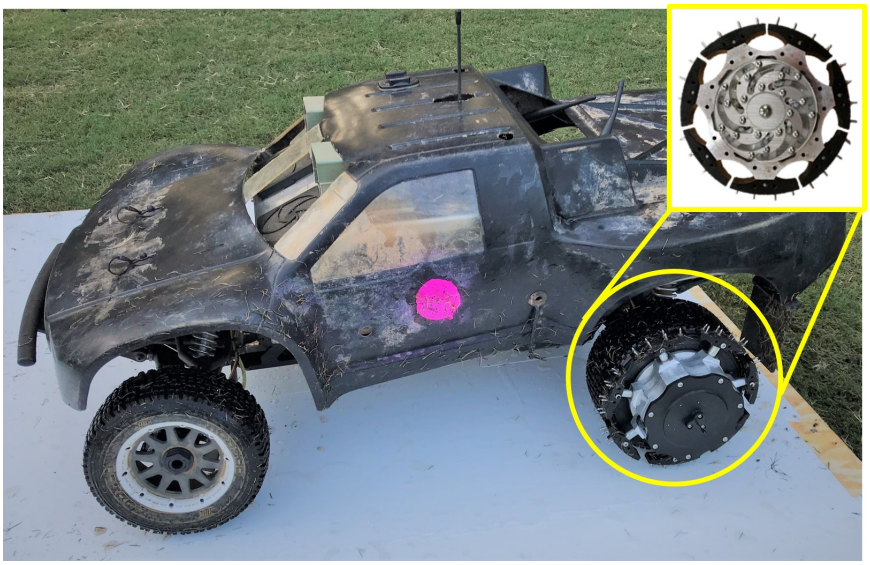

**Figure 1.2:** Traction augmentation system installed on the rear wheels of a Georgia Tech AutoRally vehicle[5].

## 1.3 Paper Structure

The remainder of this paper proceeds as follows. A set of functional requirements are outlined for friction-adaptive wheels. The resulting mechanical design is then presented and describes the new spiral-cam approach and design principles for the terrain grippers. Mathematical analysis for the cam's spiral shape and variable transmission ratio accompanies this discussion. Based on this analysis, two electromechanical prototypes were constructed and characterized on the bench level. The results validate the intended effect of spiral cam

design and demonstrate how the terrain grippers' unique geometric properties can dramatically increase friction coefficients on a range of terrains. Finally, full-scale system testing is presented that demonstrates improved vehicle maneuvering performance on the target terrains when installed onto a Georgia Tech AutoRally vehicle.

# CHAPTER 2
# FUNCTIONAL REQUIREMENTS

This section describes the functional requirements for an adaptive wheel mechanism intended for an autonomous car, truck, or buggy operating in off-road environments. For the scope of this work, the focus is on the Georgia Tech AutoRally vehicle. The vehicle is a 1:5 scale, rear-wheel-drive RC truck with a fully loaded mass of 22 kilograms [5]. The requirements are intended to be broadly applicable to accommodate use on a wide range of vehicles. Specifically, the emphasis is on designs that minimize additional mass, complexity, and power consumption, while also providing robustness to substantial wheel loads. The design should easily scale using a majority of COTS (commercial off-the-shelf) parts. Independence of scale promotes ease of installation on a wide range of existing vehicles. Using COTS parts helps to reduce overall system development effort and cost.

Particular emphasis is placed on developing a platform that modifies existing wheel configurations as opposed to outright replacement. This is a key distinction from many adaptive technologies. It is reasonable to assume that outright replacement requires a far more extensive development effort than modification. In some cases, it may be altogether unfeasible.

Based on these goals, the following requirements were set forth for the mechanism's design.

1. ***Controllable deployment***: The primary aim of the platform is to augment traction only when necessary. This means that the wheel morphology can be controlled by the vehicle's control system or remotely by the vehicle user. This differs from reflexive designs that react quickly but without selective control. Controllable deployment is essential for two reasons. One, control minimizes the risk of accidental or disadvantageous deployment. False triggers or permanent deployment can be detrimental

to the mechanism, vehicle performance, or the environment under certain circumstances. For example, studded tire technology has been shown to increase pavement wear [27] and rutting [28] while also posing health risks [29]. Secondly, terrains are rarely homogeneous. Deployment on an undesirable terrain or where mechanism performance suffers should be strictly avoided. Without a means for selective deployment, there is no guarantee the mechanism can sustain improved performance over varying terrain.

2. ***High force actuation***: Since the system is required to be controllable, the actuation system must be capable of generating sufficient forces to deploy the mechanism. For the system developed in this work, actuator effort is greatest during expansion of the friction-augmenting features. The reason is that at full expansion, the system increases the effective wheel diameter (EWD). This requires each adaptive wheel lift a fraction of the fully-loaded vehicle weight as imposed on the installation wheel. An increase in EWD is necessary to ensure complete contact of the friction-augmenting features when deployed. For the Georgia Tech AutoRally vehicle, this weight is approximately 54 Newtons per adaptive wheel.

3. ***Minimal mounting requirements***: Systems that can be readily added to a range of vehicles are highly desirable. This means that the system can easily mount to an existing wheel without replacing parts of the brakes, suspension, or drive-train. Achieving this objective minimizes the scope of the system design, minimizes system complexity, increases the attractiveness of the system to potential users, and broadens the target market for the system. This differs from the vast majority of adaptive technologies which require, at minimum, a complete replacement of the wheel itself. In practice, complete replacements are typically unfeasible and costly. An example of this is electric vehicles with in-wheel-motors [30, 31]. To be broadly applicable, the mechanism should aim to augment an existing wheel, not replace it.

4. ***Modular, configurable design***: Vehicle components in contact with terrain are subject to high levels of wear, especially during aggressive maneuvering. Furthermore, friction-augmenting surfaces can vary in form to address specific terrains [32] (i.e., deep-grooved tires on sand), and the ability to easily swap one gripping device for another is particularly desirable. Both aspects can be addressed through modular design. Should a component wear excessively, it can be easily replaced. Likewise, modular frictional (gripping) components can be interchanged to target certain terrain. The resulting design maximizes longevity and terrain-specific performance.

5. ***Unobtrusive form factor***: Mounting any mechanism to an existing wheel increases the footprint of the resulting, modified wheel. To ensure compatibility with an existing vehicle structure, the system should be compact and self-powered. Three possible locations on an existing wheel are feasible to such an approach: wheel exterior, mid-wheel, or wheel interior. Mid and interior mounting locations require that when the suspension is fully compressed (vehicle frame closest to the terrain), the mechanism's gripping elements cannot contact any existing features of the vehicles. This included the frame, vehicle body, braking system, etc. Such geometric restraints may relax with an exterior-wheel mounting location.

6. ***Low power consumption***: Advances in battery technology, propulsion, and miniaturization continues to broaden the range of missions possible by autonomous vehicles [33]. Certainly, vehicle range concerns frequently arise in passenger and commercial vehicle use [34]. The efficiency of the mechanism in converting power to improved traction performance is thus a critical component of the system's attractiveness and usefulness, as is instantaneous and sustained power draw.

   Since the system is ideally compact and self-powered, it must have low power consumption. Compactness, in this sense, reduces the inertial burden in performing aggressive vehicle maneuvers like rapid accelerations. It concomitantly achieves re-

duced mass. Power storage independent of the vehicle is important to mechanism/ vehicle compatibility and may contribute to system robustness by circumventing wear-prone hardware like slip rings.

Since the system will largely exist in either the deployed or stowed configurations, in both cases, the actuators should not be required to maintain posture. Actuator power should only be used when changing the configuration of the mechanism. Thus, power consumption is minimized and results in lower actuator run-time to promote greater longevity.

Finally, the sensor package required to operate the system ideally utilizes few and low-power or passive sensors. While most modern, active sensors feature low-power modes, their power consumption performance cannot match that of most passive sensors properly integrated into a circuit. Additionally, passive sensors are generally more robust, cost-effective, and have better working life than active sensors.

7. ***Robustness to external loads***: Off-road driving can induce large forces and accelerations, especially when the terrain is rough and differs widely. The most detrimental source of failure is shock-loading, in which the magnitude of the load reacted through a wheel can be many times greater than the distributed weight of the vehicle. Deriving from the resulting impulse of an event, the force magnitude largely depends on the stiffness of the vehicle suspension, which is predetermined for an existing vehicle. Changes to suspension are assumed unfeasible. Other potential deleterious factors include heavy vibration, transverse torsional loading from turning and cornering, and increased torque transfer from drive train to terrain as enabled by increased traction. With controllable mechanisms that must react such external loads, the actuator is frequently a failure mode. Thus, methods that protect or shield the actuator from terrain-induced loads can greatly enhance robustness.

A review of existing literature failed to provide a solution that completely meets this

set of requirements, especially for a scaled vehicle. For instance, static and quasi-static solutions like tire chains are generally low-profile, easily mounted, minimize vehicle power consumption, and are highly robust; but, they cannot be controllably deployed and stowed. Passive traction technologies also lack this feature. Controllable deployment is essential to expanding the traction capabilities across a wide variety of terrains and allows the vehicle to select the most suitable gripping feature (tire or terrain gripper) for current conditions.

Active technologies that morph or feature articulating structures to aid in locomotion, on the other hand, are controllable. Yet, the bulk of these are targeted at traversing obstacles. Utilizing legs or whegs is a prime example of this operation scheme [35–37]. While many such systems afford use of a wheel to promote efficiency on flat terrain, the wheel's traction is not the central focus. Ice is a good example. If the wheel's traction is not specifically addressed, it cannot be expected to adequately enable aggressive vehicle maneuvering.

Active systems are, in general, at risk of premature failure and may lack in efficiency. For instance, systems that require actuator effort to maintain posture suffer from constant power draw. Long-range missions usually reserved for wheeled-vehicles cannot be reasonably conducted with these systems. This configuration also places undue stress on the actuators. Heavy shock loads arising from variations in terrain may be transferred directly through a backdrivable drive train to increase the incidence of actuator failure. Efforts may be taken to shied the actuator [37] but can still leave gearing exposed.

Complexity also tends to be an issue. Two general types are of concern: 1) overall mechanism complexity and, 2) mounting complexity. Highly complex mechanisms naturally introduce many potential failure modes. Unique or expansive geometric features also make environmental sealing or shielding difficult. Off-road environments are particularly inhospitable to unshielded electronics, actuators, and gears due to an abundance of potential contaminants. Complexity in adapting to existing vehicles, for many of the surveyed systems, also requires complete replacement of the wheel because of their unique

design. For existing vehicles utilizing rubber tires, adaptation is troublesome or unfeasible given the additional development effort required to mate with the existing body, frame, or suspension.

Notwithstanding these difficulties, a potential solution has been highlighted in the media [38]. However, such reports fail to provide details regarding functional requirements, electromechanical design, or technical performance. It is therefore difficult to assess the merits of such a design until relevant engineering details are forthcoming. Perhaps the most relevant existing method is the ability to switch between wheeled and tracked locomotion [22, 23]. This system differs from the approach taken because it changes the mode of locomotion and is currently focused on implementation on large-scale vehicles.

The approach adopted in this work maintains the locomotion mode, utilizes a hub-mounted spiral cam for selective deployment, and exploits a singular configuration for energy efficiency and robustness. This system can be controllably actuated using a small electric motor, easily mounts to an existing wheel with few and simple components, consumes minimal power when stowed and fully deployed, is environmentally sealed, and is able to protect the sensitive components of the drive train from harsh driving conditions.

# CHAPTER 3

# MECHANISM DESIGN

The overall mechanism design framework for this work is shown in Fig. 3.1. The design utilizes high-friction grippers to dramatically increase the coefficient of friction on a set of target terrains. For the remainder of this paper, such high friction surfaces are referred to as *terrain grippers* or grippers for short.

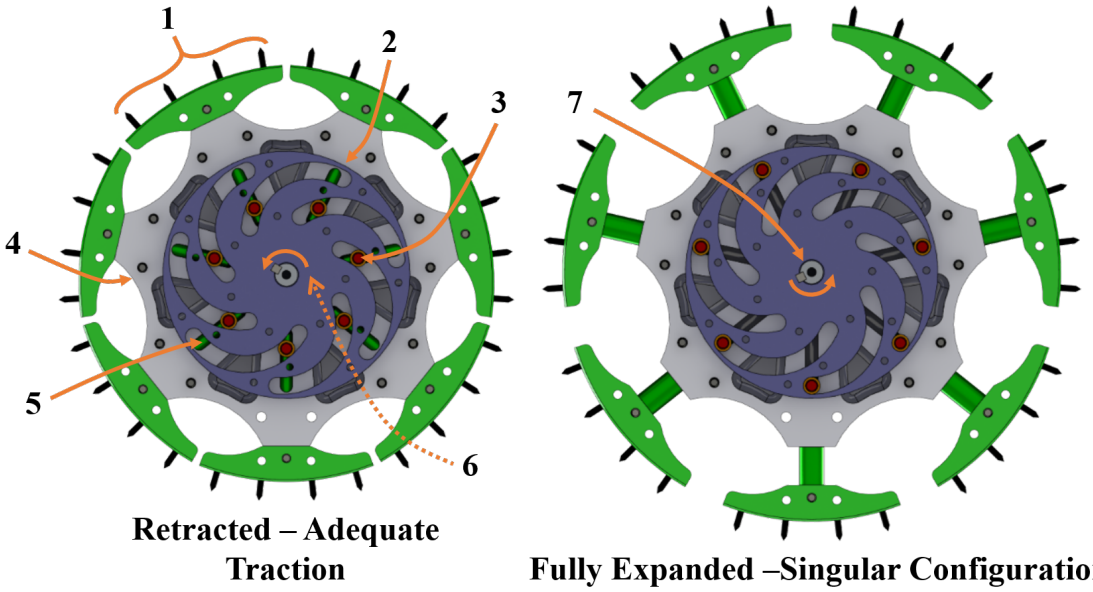


**Figure 3.1:** Annotated mechanism with retracted to extended configurations: 1. Terrain gripper, 2. Spiral cam, 3. Guide pin, 4. Wheel-mount, 5. Wheel mount linear pockets, 6. Cam-extending rotation direction, 7. Central drive shaft.

The mechanism modulates wheel traction by deploying its set of grippers. To deploy the grippers, rotational input motion is generated by an on-board motor and transferred to the spiral cam mechanism through the central drive shaft. The spiral cam converts the rotation to linear output motion of each gripper's linear shaft. Seated at the radial extreme of each linear shaft is the gripper body and is connected by a single fastener. Coupling between cam and linear shaft is achieved by way of a guide pin. The terrain grippers can be

made to extend and retract through this design, thereby allowing controllable contact with the terrain.

A unique feature of a vehicle modified by this system is the ability to utilize both the grippers and original vehicle tires. Expanded, the grippers exclusively engage the terrain. Retraction, on the other hand, renders the grippers inactive with respect to the terrain, allowing the rubber tire to operate unaided. The ability to select between gripper and tire is an important feature of the design because it expands the traction performance of the modified wheel. Whereas the gripper is designed to outperform on a set of target terrains, the rubber tire may outperform on another set of terrains. For instance, modern rubber tires have been engineered to perform well on dry pavement but degrade in performance when the pavement is wet, contaminated (i.e. loose media like sand or gravel is present), or covered in ice or snow [39]. A deployable gripper designed to address such adverse conditions is easily seen to expand the traction performance of the tire.

The majority of the system's components reside exclusively within the wheel mount. This includes the actuator, electronic suite, and transmission (which includes the spiral cam). Component isolation in this manner allows environmentally sensitive components to be sealed within the wheel mount. This is important to the overall robustness and longevity of the system. Only the mechanically simple terrain grippers and wheel mount are exposed to the environment.

A subtle, yet significant, aspect of the design is the ability to easily mount to the exterior of the wheel. Specifically, the wheel rim of most off-road vehicle wheels can be mounted to. This location is ideal because it limits the effort required to mount to an existing wheel, requiring a simple adapter plate to fix the mechanism to a wheel. The adapter serves only to structurally connect the wheel mount to the rim to transfer vehicle loads from gripper to wheel. Further modifications to the wheel or adjoining structures are not required. In this configuration, the potential of the mechanism to interfere with the vehicle structure, notably the vehicle body, is minimized.

The overall system can thus been simplified into two core subsystems: 1) terrain grippers, and 2) the expansion/retraction mechanism. The design of these subsystems are described in the sections that follow.

## 3.1 Terrain Gripper (*High Friction Surface*)

In this work, three candidate off-road surfaces were targeted for friction enhancement: 1) ice, 2) grass, and 3) dry, packed dirt. Such selections were based primarily on availability for testing and ubiquity in off-road settings. The driving feature of these terrains, however, was relatively poor performance when conducting aggressive maneuvers with scaled vehicles. High accelerations and hard turns tend to produce wheel slip that degrades performance. To enable more aggressive control, more aggressive traction-augmenting technologies needed development.

The modern tire is selected as the performance benchmark due to its widespread deployment on wheeled, ground-base vehicles operating on all types of terrain. To maintain generality, no distinction is made between varying types of tire configurations. Certainly, a wide variety of configurations exist to address a plethora of design goals[40]. The underlying frictional mechanics, however, remain largely the same.

### 3.1.1 Traction Mechanics

Traction describes the grip a feature experiences with another surface. Really, traction is a generalization of friction as it applies to the terrain-contacting components of a vehicle on a particular terrain. It also tends to be a description of relative motion between contacting surfaces. Whereas *good* traction is usually defined by the condition of zero relative surface velocity, *poor* traction or loss of traction exhibits a difference in velocity of the gripping element or elements relative to its operating surface, which here is assumed fixed. While quantitative, this perception of traction quality is important. Wheels and tracks operate most effectively when in rolling contact with their terrain, the incidence of which requires

that the acceleration/deceleration demands imposed by the vehicle drive train not exceed the available static friction at the wheel/terrain interface. With this in mind, the focus here is on influencing static friction and not kinetic friction, although the two types are inherently related and occur to varying degrees simultaneously [41].

*Small-Scale (Micro) Friction*

Physically, all surfaces are rough at some scale. As illustrated in Fig. 3.2, this roughness can be observed as a web of jagged features; it is also the basis for adhesion. A normal load, $N$, compressing two surfaces together causes distortion of one or both surfaces into these jagged features, or surface asperities, thereby creating mechanical interlock and increased contact area between the surfaces. Distortion can be visco-elastic or elasto-plastic in nature, depending on the materials involved. Adhesion produces grip through a number of interactions taking place simultaneously. Mechanical adhesion derives from the simple interlocking of asperities. Chemical adhesion arises from covalent, ionic, or hydrogen bonding of the areas of contact, or *real contact area*. Dispersive adhesion involves Van der Walls forces. In general, however, mechanical adhesion is the only type that produces substantial friction at a variety of scales. For instance, chemical and dispersive interactions exist on the micro and nano-meter scales and therefore require close conformance of surfaces.

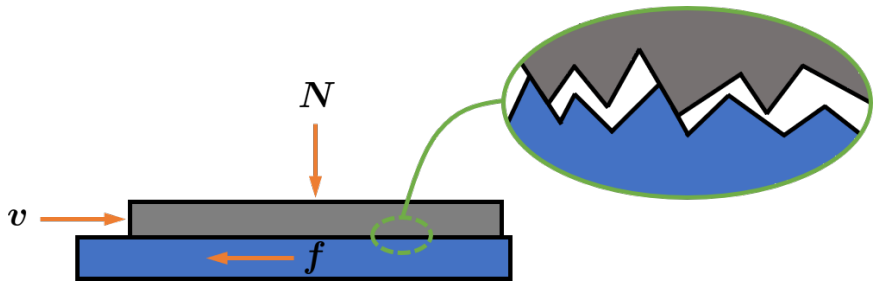


**Figure 3.2:** Scaled surface interaction of hard surfaces.

A logical extension of this discussion is that adhesive friction can be increased by pro-

moting greater development of real contact area. A corresponding method to achieve this is utilization of a more compliant gripping element. Elastomers (including tires) accomplish this task and, in addition to adhesion, tend to exhibit appreciable friction from hysteresis [42–44]. An illustration of these interactions is given in Fig. 3.3. Hysteresis friction derives from the bulk deformation of the material on a harder contact surface like asphalt. As the tire rotates to contact fresh pavement, pressure forms as the tire conforms to surface asperities. It is this pressure that produces additional frictional resistance.

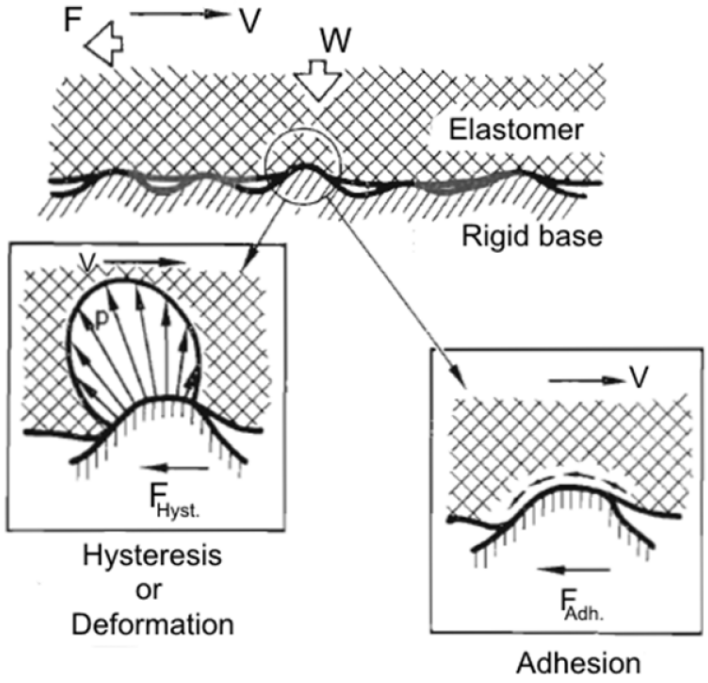


**Figure 3.3:** Compliant material (elastomer) frictional interaction with rigid terrain.

In general engineering practice, a common working model for friction is known as Coulomb friction [45], as given by Eq. (3.1). The model provides a simple relation between the friction force, $f$, the coefficient of friction, $\mu$, the normal compressive force acting at the surface interface, $N$, and the sign, *sgn* of the sliding velocity, $v$.

$$f = \mu N \text{sgn}(v) \tag{3.1}$$

Coulomb friction is an empirical description of friction. The implication of Eq. (3.1) is that friction is a function of real contact area and the limiting (or lower) interfacial shear stress. A physical interpretation aids the point. For a given normal compressive force, some amount of real contact area results. Eq. (3.1) implies that greater normal force produces a roughly proportional increase in real contact area and thus, assuming the limiting shear stress remains unchanged, proportionally greater holding force.

An immediate mathematical and computational issue with the Coulomb friction model is the discontinuity at zero velocity [46]. It also fails to incorporate viscous damping and other notable phenomena (i.e., *Stribeck Effect*). The issue from zero-velocity continuity may be alleviated by introducing a smoothing function, $s(v, a)$, such as that given in Eq. (3.2) [45]. In Eq. (3.2), $a$ is a coefficient specific to the interaction of the contacting surfaces. The remaining issues may be dealt with by incorporating terms for the viscous friction coefficient, $\sigma_v$, and a general function for the Stribeck effect, $F_s(v)$ [47]. The resulting, modified equation is given in Eq. (3.3).

$$f = \mu N \text{sgn}(v) s(v, a) \tag{3.2}$$

$$f = \mu N \text{sgn}(v) s(v, a) + \sigma_v v + F_s(v) \tag{3.3}$$

This expanded model provides a useful (albeit oversimplified and error prone) predictive basis for gripper design in the presence of gross slippage. However, the goal in designing a gripper is to ensure static contact. For $v \approx 0$, the original Coulomb model results. Despite the limitations of the Coulomb model, its simplicity is attractive. It allows for quick calculation of a coefficient of friction to evaluate candidate grippers by. As long as the increase in the friction coefficient afforded by a gripper is great enough relative to the benchmark tire, modest errors are permissible. Further discussion is presented in the *Results* section.

*Large-Scale (Macro) Friction*

The frictional processes described thus far can be characterized by a lack of damage and wear to either surface. They also tend to occur on relatively small scales. Contrast this with gouging or indentation of one surface into another, such as the action of a tire indenting snow [48], and a macroscopic avenue to creating holding force arises. If a gripper is sufficiently hard with respect to the terrain and makes contact with sufficient pressure, it will create mechanical interference through indentation. The holding force is then largely a function of terrain shear stress, $\sigma_s$, and cross-sectional indentation area, $A$ (measure perpendicular to the direction of instantaneous wheel loading). A simplified representation of the holding force, $F_h$, is presented in Eq. 3.4. Note that the frictional interface is assumed to be static and that $\sigma_s$ represents the lower of the two contacting material strengths.

$$F_h \propto \sum_{i=1}^{n} A_i \sigma_s \tag{3.4}$$

Based on Eq. (3.4), increased grip may be achieved through more indentations or increased indentation area, as indicated by [49]. Both can be achieved simultaneously with a more compliant gripper. A greater number of indentations is desirable because it reduces the linear force burden on each interaction; lower force burden then reduces the tendency of the indented feature to deflect from a surface asperity. Indentation area, on the other hand, defines the product of indentation depth, $h$, and width, $w$, the latter of which is measured perpendicular to the wheel's instantaneous direction of loading. Increased indentation area contributes to terrain strength because for a given load, increased area reduces stress on the indented area. For compliant materials, indentation volume is a more appropriate indicator of expected performance because it implicitly incorporates a stiffness element: the depth of the indent parallel to wheel load. However, cross-sectional area is highlighted here because the gripper design utilizes rigid indenters such that the indented-feature stiffness is implicit. This also means that the failure (incidence of slippage) is assumed to derive from

the terrain and not the indenter.

Holding force is thus based on terrain strength, and indentation area is critical to terrain strength. In other words, terrain failure becomes the primary factor influencing frictional slippage. Fig. 3.4 provides a framework for two possible terrain failure modes: terrain shear and vehicle lift. For grass and dry-packed dirt, the Mohr-Coulomb failure criterion provides a good approximation of the onset of failure. Represented by Eq. (3.5), the amount of torque-generated linear force, $F_T$, that can be withstood by the terrain before a section of terrain shears is dependent on the cohesion of the soil, $c$, the indentor cross-sectional area, $A = wh$, and the angle of internal friction, $\alpha$. The indentor is assumed to be perfectly rigid, failure occurs along a shear plane, and the static friction along the leading indentor/terrain contact is not overcome by indenter lift.

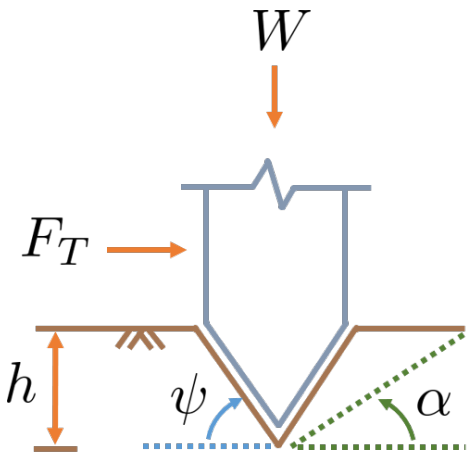


**Figure 3.4:** Framework for static terrain failure from interaction with an arbitrary indenter.

$$F_T = \frac{2cwhcos(\alpha)}{1 - sin(\alpha)cos(\alpha)} \tag{3.5}$$

The second failure mode assumes the indenter is forced out of its indent, leaving the terrain largely intact. This assumption is reasonable for mechanically strong, low friction surfaces like ice. In this case, holding force is a function of the indenter contact angle, $\phi$, the indenter/surface coefficient of friction, $\mu$, and the vehicle weight pressing the indenter into

the terrain, $W$. Noting the reliance on Coulomb friction, the relation is given in Eq. (3.6).

$$F_T = \frac{W(sin(\phi) + \mu cos(\phi))}{cos(\phi) - \mu sin(\phi)} \tag{3.6}$$

Both failure modes discussed assume the terrain exhibits reasonable cohesion and that the indented regions are of relatively low quantity and discrete. This poses difficulty when the terrain is highly deformable. Pressure-sinkage theory can be used to calculate wheel forces at the contact patch in such cases. As discussed later, however, the method used to augment traction adopted in this work focuses exclusively on discrete indentation on rigid terrain. For more information on deformable terrain calculations, the reader is referred to [50].

### 3.1.2 Augmenting Technologies

Commonly available technologies for friction enhancement are exclusively static or quasi-static. Static technologies targeted for on-road use include specially formulated rubbers, specific tire geometries [49], and tires with embedded features. For instance, "winter tires" exhibit low glass-transition temperatures and may contain specific additives like silica to improve wear resistance. The effect is greater compliance at low temperatures to allow for greater development of real contact area. Testing has demonstrated dramatic improvements in friction coefficients in cold weather [40]. Geometric features that contribute to friction include special pattern block and sipes (small-scale channels cut into pattern blocks). On frozen terrains, these features combine to displace in-situ fluids to increase indentation [49], as represented by Fig. 3.5. Embedded features, on the other hand, are generally restrained to studs of differing geometry that promote indentation on hard surfaces like ice.

Despite their typical on-road application, such on-road technologies may be deployed off-road to good effect. In exclusively off-road environments, wide, large-diameter tires with deep, spacious grooves are common [51]. The general effect of such geometry is an increase in real contact area and greater contact pressure uniformity. While tracks may also

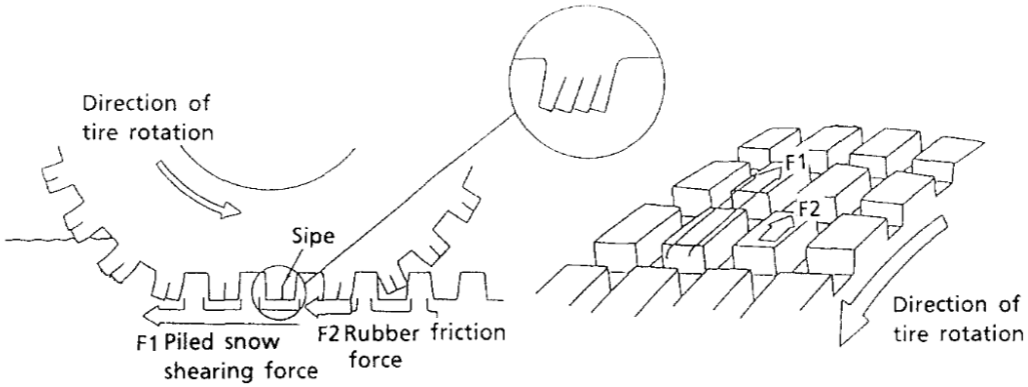


**Figure 3.5:** The effect of tread pattern design on frozen terrains [49].

be included in this group, this work focuses exclusively on wheel-based vehicles.

Typical quasi-static technologies include removable chains, socks, and sleds largely intended for driving on snow and ice. The method of improving traction varies by design. For example, steel chains are designed to provide large-scale indentation on snow and ice. Contact area is developed exclusively between chain and terrain; being of lesser magnitude, reduced contact area develops greater contact pressure to provide "bite." Alternatively, socks exhibit greater conformance to terrain than tires at low temperatures to increase real contact area.

### 3.1.3 Insights and Gripper Design

Based on the foregoing discussion, gripper design starts with a consideration of scale. Effective small-scale friction relies on a maximization of real contact area between the gripper and terrain asperities. Grip, depending on the fractal nature of the surface, is a function of adhesion and deformation (hysteresis) [52]. Macro-scale friction involves penetration of gripper features into the terrain and therefore derives almost exclusively from mechanical interference (Fig. 3.6). Properly designed, macro penetration can also circumvent sources of performance degradation that compliant methods cannot, such as adverse surface conditions (contamination, wetting, etc.).

Micro-scale traction methods are not without merit. A natural conclusion to draw from

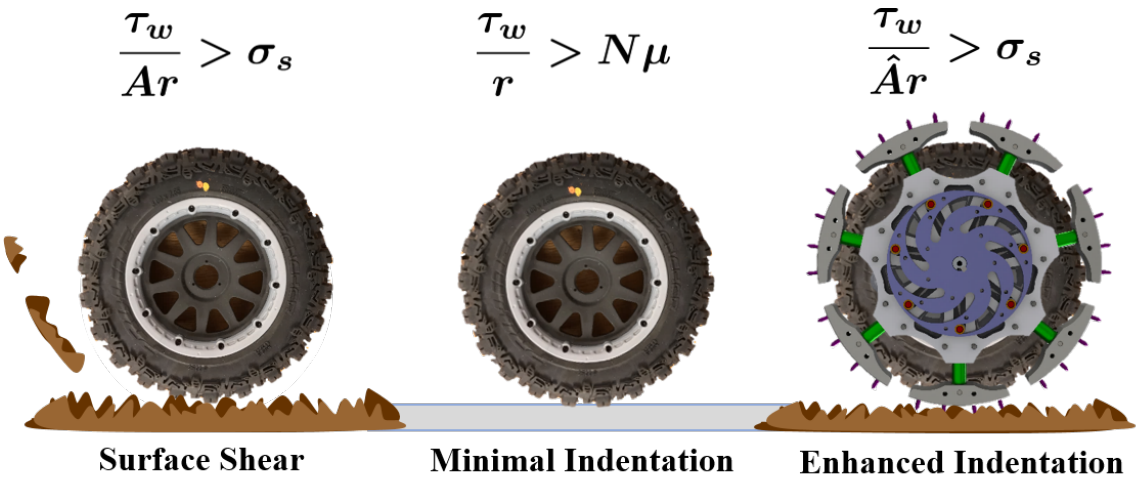


**Figure 3.6:** Selection of a suitable terrain gripper relies primarily on its indentation capacity and the nature of the terrain. This figure presents three wheel slip scenarios with corresponding slip conditions, where $\tau_w$ is wheel torque, $A$ indentation area, $r$ wheel radius, $\sigma_s$ terrain strength, $\mu$ static friction coefficient, $N$ normal force, and $\hat{A}$ mechanism-enhanced indentation area.

the relationship between traction and real contact area is that improved traction can be achieved with a more compliant material, as discussed previously. A similar effect results from reducing the pressure in pneumatic tires. However, utilizing compliance may not provide benefit for all conditions. In general, compliant materials have lower strengths and may sacrifice in longevity unless special compounds are added to their chemical formulations. Such an approach also neglects the effect of surface lubrication. Highly compliant contact can trap water in surface asperities to severely inhibit indentation [53]. Trapped fluid reduces the effective pressure between tire and terrain by introducing hydrostatic pressure, resulting in the development of less real contact area and an appreciable reduction in friction. Other common effects include boundary and hydrodynamic lubrication [52], the latter of which is of particular concern during high speed vehicle maneuvers. Compliant gripping elements must therefore draw a balance between desirable traits like fluid displacement, compliance over a range of temperatures, and wear resistance. They also tend to be be geometrically complex, difficult to procure or manufacture, and potentially expensive for use in a prototype.

Such limitations rarely apply to macro methods. If inducing surface damage is acceptable, as is often the case in off-road settings, indentation is easily achieved by employing sharp features. Options include blades, spikes, teeth, and other similar elements sharpened to reduce the contact area. A natural tradeoff exists between the number of sharp features per gripper, penetration depth, relative acceptable sharpness, and structural integrity of the gripping element that must be considered in the design.

The solution employed here aims to provide appreciable indentation on a variety of terrains. To puncture surfaces like ice, cylindrical pins are sharpened to create spikes. An array of spikes is then assembled to create an enhanced-friction surface. The configuration of the array depends on the desired performance. In this design, the spikes form two symmetric, equally-spaced rows installed on a partial arc. This approach draws a relatively equal balance between expected indentation area, spike structural integrity, and anticipated wear performance. To protect the gripper body (the partial arc) from damage during overloading events, the pins are pressed into sacrificial nylon sleeves that are pressed into holes in the gripper body. The resulting terrain gripper is are shown in Fig. 3.7.

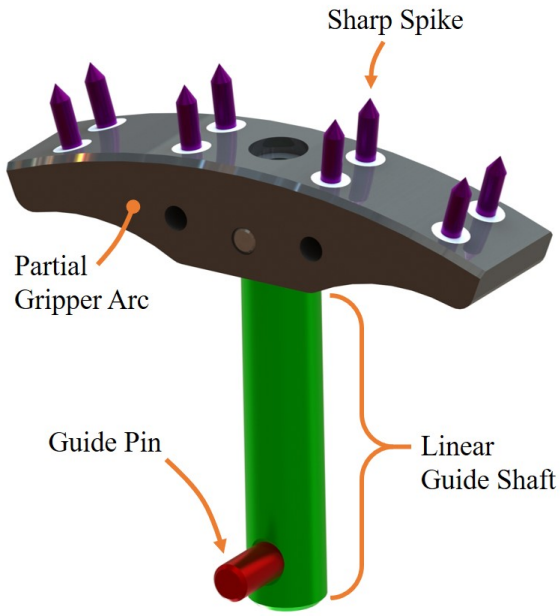


**Figure 3.7:** Terrain gripper design with sharpened spike.

Alternative configurations exist to optimize any given performance metric. For example, a staggered arrangement may minimize material accumulation on a gripper at the expense of structural integrity (one spike may be required to transfer wheel loads to the terrain). However, reducing accumulation was not considered essential in this work. The chosen configuration produces acceptable indentation on a wide variety of surfaces and is independent of the wetting condition of the surface. The inherent drawback is that to remain effective across all terrains, particularly ice, the spikes must stay sharp. As demonstrated in the *Results* section, blunting of the spikes reverses performance gains on ice.

## 3.2 Expansion Mechanism (*Spiral Cam*)

To controllably deploy a set of terrain grippers, a compact method for expanding and retracting the grippers is necessary. Theoretically, any reasonable combination of actuator and gearing can accomplish this task. Since rotary, electromagnetic actuators are readily available, compact, and easy to control, a mechanism that converts input rotary motion to linear output motion provides considerable advantages. The "spiral cam" was developed for this purpose and offers a unique set of tunable features. Its most immediate advantage is minimal height. Depending on the number of desired grippers (which determines the number of spiral cam slots), the spiral cam can be easily designed to carry the full allottable vehicle load on its installation wheel at very little thickness. Low height is desirable to reduce the additional footprint, mass, and cost of the overall mechanism.

The methodology employed is shown in Fig. 3.1. In Fig. 3.1, the "wheel mount" (gray) is connected directly to the wheel. The spiral cam consists of a series of slots that interact with the guide pin on each terrain gripper. This means that the number of spiral cam slots always equals the number of terrain grippers. Rotary input from a drive motor is converted to radial, linear extension/retraction of each terrain gripper (green). From the initial, retracted state, motor torque rotates the spiral cam slots (purple) into contact with the guide pins (red) of each terrain gripper. The resulting contact angle imposes an outward

radial force, or expansion force, $F_E$, relative to the wheel mount center. Since the guide pins are fixed to the terrain grippers, the grippers are forced out radially relative to the wheel mount center. To enable purely linear motion of the grippers, the guide pins are also constrained to move within linear pockets in the wheel mount. The following section defines the input/output characteristics of the spiral cam geometry mathematically.

### 3.2.1 Input-Output Model

For this discussion, it is assumed that the wheel is temporarily stationary. The input-output behavior of the spiral cam can be tuned based on speed, force, or packaging requirements. The analysis presented here focuses on the input-output behavior of a single cam slot. As Fig. 3.8 illustrates, the shape of each cam slot is a circular arc of radius $R$. The center of each such arc is offset from the input motion's axis of rotation by displacements $x_c$ and $y_c$. By offsetting the path center, an angle, $\theta(\psi)$, develops between the position vectors $\vec{h}(\psi)$ and $\vec{p}(\psi)$. These vectors are shown in Fig. 3.8 and represent the vector connecting the cam slot and the input axis of rotation, $\vec{h}(\psi)$, and the vector connecting the cam slot and the center of the cam slot arc, $\vec{p}(\psi)$. Location along the path is defined by the path angle, $\psi$. The magnitude of $\vec{h}(\psi)$ and $\vec{p}(\psi)$ are defined as as $|\vec{h}|$ and $|\vec{p}|$, respectively.

$$\vec{h}(\psi) = \langle R\cos(\psi) + x_c,\ R\sin(\psi) + y_c \rangle \tag{3.7}$$

$$\vec{p}(\psi) = \langle R\cos(\psi),\ R\sin(\psi) \rangle \tag{3.8}$$

$$\cos(\theta(\psi)) = \frac{\vec{h}\cdot\vec{p}}{|\vec{h}||p|} \implies \theta(\psi) = \cos^{-1}\left(\frac{\vec{h}\cdot\vec{p}}{|\vec{h}|R}\right) \tag{3.9}$$

The angle, $\theta(\psi)$, defines the kinematic relationship between the tangential cam slot velocity, $v_T$, and the output guide pin radial velocity, $v_r$. The relationship between $v_T$ and

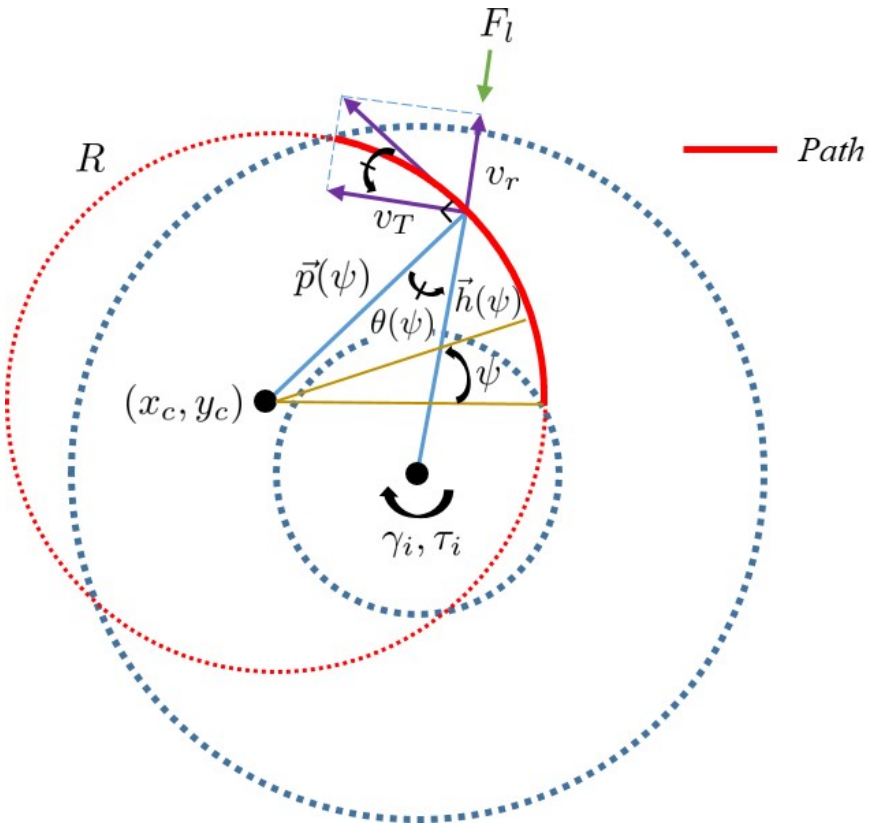


**Figure 3.8:** Spiral cam geometric design framework.

the angular velocity of the cam, $\dot{\gamma}$, is given by EEq. (3.10).

$$v_r = \dot{\gamma}|\vec{h}|\tan(\theta(\psi)) \tag{3.10}$$

The system can be treated as a rotary-linear transmission with input-output ratio, $N$. Note that the system has a variable transmission ratio that changes non-linearly with configuration. Since power is converted from radial to linear, the units of $N$ contain a length dimension.

$$N = \frac{\dot{\gamma}}{v_r} = \frac{1}{|\vec{h}|\tan\theta(\psi))} \tag{3.11}$$

Energy losses in the mechanism are minimized by utilizing either lubricated bushings or ball bearings on all moving parts in the mechanism. Assuming losses to be negligible, conservation of energy can be used in combination with Eq. (3.10) to determine the ki-

netic relationship between rotary input and linear output. Of particular interest is the input torque, $\tau_i$, that is required to overcome the local linear load, $F_l$, to fully extend the grippers out radially.

$$\tau_i = \frac{v_r F_l}{\dot{\gamma}} = F_l |\vec{h}| \tan(\theta(\psi)) = \frac{F_l}{N} \tag{3.12}$$

For this application, the spiral cam geometry must satisfy two core requirements. First, the transmission ratio, $N$, must remain relatively small over much of the range in $\psi$. This promotes rapid deployment of the grippers. Additionally, once fully deployed, the system must bear steady loads (such as the vehicle weight) without consuming actuator power. Therefore, for large $\gamma$, the transmission ratio ideally approaches infinity. This is known as a singular configuration and means that forces imposed on the terrain grippers can be withstood with zero reactive actuator torque. Essentially, the grippers are effortlessly *locked* in an expanded configuration until the actuator draws the grippers into a retracted position again. This "lockout" is important for robust gripper deployment on rough terrain where loads imposed on the gripper can be intermittent and of large magnitude. Such a configuration, coupled with a carefully engineered path geometry, affords the use of a relatively small motor to lift the vehicle.

### 3.2.2 Design Principles

The use of a tailored spiral cam geometry is a key contribution of this work, and has two core benefits. First, no input actuator power is needed once the mechanism is deployed. Second, the actuator and drive train is shielded from high loads imposed by the terrain, thereby enhancing longevity. Note that vehicle loads are transferred directly to the spiral cam through the gripper guide pins and terminate at the central drive shaft. Fig. 3.9 provides an illustration of the load path. To safely react such loads, a minimum critical spacing must be maintained between spiral cam slots. Also, the drive shaft and guide pins must be of sufficient diameter. Increasing the drive shaft diameter is relatively easy to ac-

complish. Maintaining proper slot spacing and ensuring adequate guide pin diameter is more involved and requires consideration of several factors, as explained below. In some cases, critical spacing requirements can be reduced through the use of a *backer-plate* that provides structural support to the spiral cam.

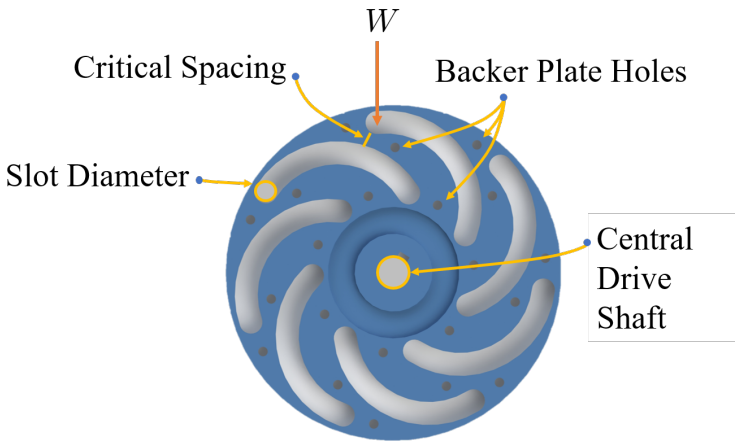


**Figure 3.9:** Development of a singular configuration causes axial wheel loads, $W$, to react through the spiral cam without transferring torque to the rest of the drive train.

Design of the spiral cam begins with selection of a suitable path geometry (see Fig. 3.8). The choice need not be limited to a circle, and a variety of curvilinear geometries may be utilized to elicit the desired performance. In general, it is desirable that the terrain grippers collectively behave like a continuous wheel. Therefore, maximizing the number of grippers resembles an initial design goal. Noting that each gripper's guide pin and cam-slot must fully react any axial loading through the gripper, load capacity is a function of guide pin diameter, and increased guide pin diameter reduces critical spacing, an upper limit on gripper count is imposed for reasons of structural integrity. Fig. 3.9 illustrates this structural requirement as *critical spacing*. In the prototype created, a maximum of 7 grippers could be safely utilized.

Definition of the number of grippers thereby defines the number of slots that must be cut into the spiral cam. To most effectively utilize space, it was desirable to place the cam on the interior of the mechanism, within the wheel recess. The recess constrains the outer diameter of the cam to a maximum given by $d_o$. An inner diameter constraint, $d_i$, must also

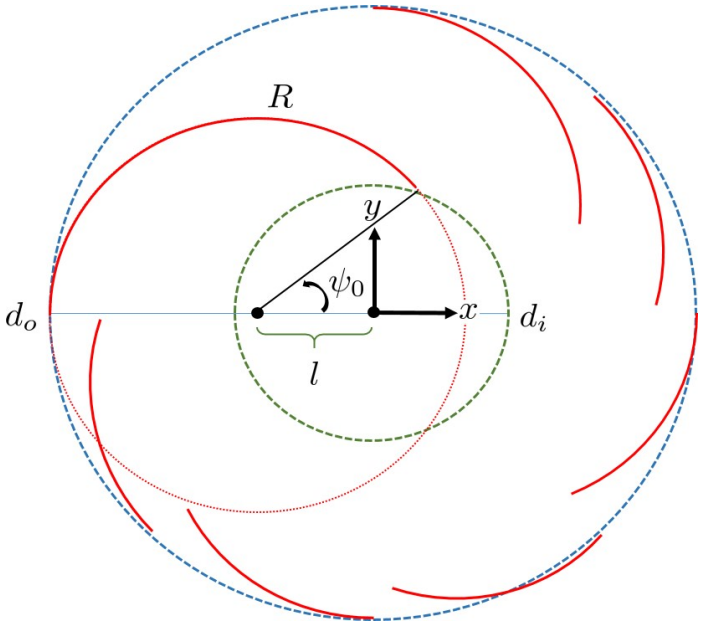


**Figure 3.10:** Selection of spiral geometry (red line) depends on inner diameter (green-dashed line) and outer diameter (blue-dashed line) constraints. The spiral offset, $l$, and permissible spiral radii, $R$, are thereby constrained. Note that all but one spiral path are visually truncated to improve readability.

be imposed on the circle intersecting the slots' innermost radial positions (at $\psi_0$) to prevent guide shaft collisions. This constraint is based on the diameter of the terrain gripper's guide shaft, the latter of which is a function of the anticipated loads imposed by the vehicle during operation.

The circular slot naturally stems from $d_i$ and $d_o$. An inherent advantage is that the angle defining the spiral cam transmission ratio, $\theta$, can be designed to gradually reach zero at the end of the path. If the path center is offset only in $x$ *or* $y$ (but not both), the path becomes tangential to a circle connecting the path ends when $\psi = 180°$. This is true as long as the offset, $l$, satisfies Eq. (3.13). Selecting an offset fixes the slot radius, $R$, per Eq. (3.14). Alternatively, one may first select $R$ per Eq. (3.15), whereby $l$ is fixed via Eq. (3.14). Fig. 3.10 provides a visual of these constraints. Note the relationship between offset and slot radius: at maximum offset, the slot radius is minimized. Conversely, radius

is maximal at the minimum offset.

$$\frac{d_o - d_i}{4} \leq l \leq \frac{d_o + d_i}{4} \tag{3.13}$$

$$R_o = R + l \tag{3.14}$$

$$\frac{d_o - d_i}{4} \leq R \leq \frac{d_o + d_i}{4} \tag{3.15}$$

As can be seen in Fig. 3.11, the transmission ratio designed with these criteria produces the desired qualities. Along the majority of the circular slot, the transmission ratio remains low to enable relatively rapid gripper movement. At the end of the movement, the transmission ratio approaches infinity. In order to tune the shape of the transmission ratio curve, the parameters $R$ or $l$ may be altered within the confines of Eqs. (3.13) to (3.15). If more freedom is required, $d_i$ may be increased above the minimum imposed by the guide shafts, but may not exceed $d_o$. Increasing $d_i$ with $d_o$ fixed, however, reduces the available linear stroke of the gripper, $x_g$, as shown in Eq. (3.16).

$$x_g = \frac{d_o - d_i}{2} \tag{3.16}$$

Further flexibility in curve shaping is afforded by relaxing the offset constraints such that both $x_c$ and $y_c$ can be nonzero. Adding both component offsets necessarily removes the ability to reach a singular configuration at the end of the spiral cam slot path, which may be of interest to the designer in some cases. One may also reduce the number of terrain grippers such that the cam slots span increasingly greater angles; doing so corresponds to an increase in path radius, $R$. If these efforts are still insufficient, one may explore other curvilinear paths like the Archimedes spiral or elliptical geometry, for example.

Two potential drawbacks are inherent to the approach described. Maximizing the num-

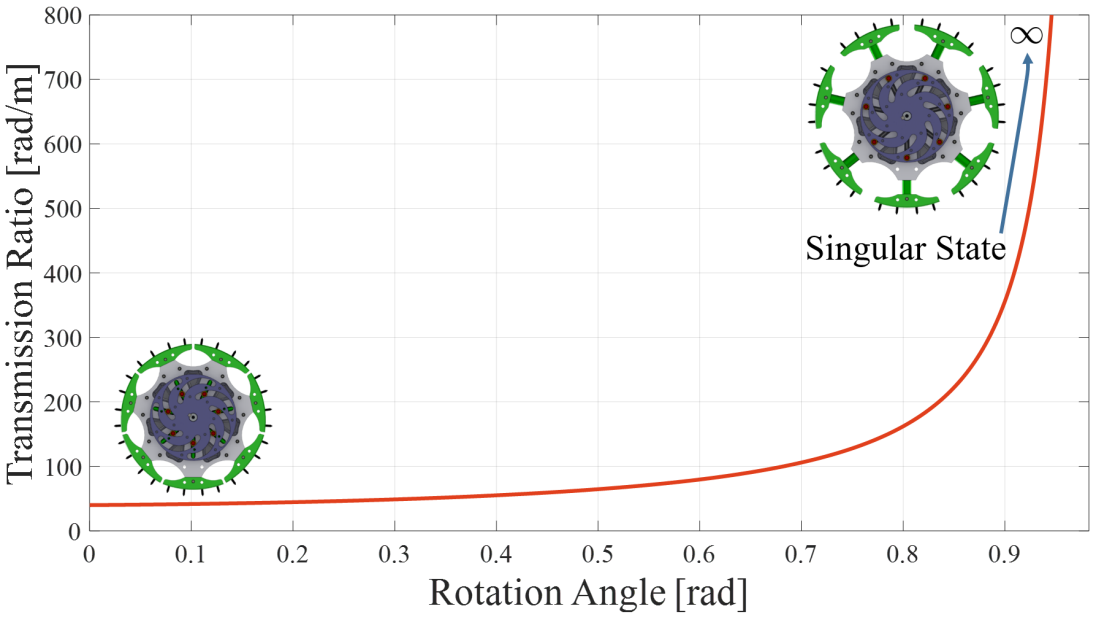


**Figure 3.11:** Spiral cam transmission ratio showing end-of-path singular behavior.

ber of grippers increases mechanism complexity and potentially reduces robustness. Secondly, the controllable aspect of the overall design introduces unique failure modes. Notably, acute material accumulation between any gripper and the mechanism hub can prevent retraction of the gripper. Additional considerations to prevent such accumulation (i.e. an expandable mesh) may be warranted in some use cases but are not explicitly addressed in this work.

### 3.2.3 Design Process

In general, the process of spiral cam design can be condensed in a series of basic steps. It is assumed that the slot geometry is the circular arc, as discussed in this section.

1. Select a suitable number of terrain grippers to be deployed by the spiral cam.

2. Select either the path offset, $l$, or the slot radius, $R$, to satisfy deployment speed/actuator requirements.

3. Ensure the critical spacing, guide pin diameter, and guide shaft safely provides support for anticipated wheel loads. If the results are unsatisfactory, return to Step 1 to

reduce gripper count.

4. Reduce the slot radius, $R$, or increase the path offset, $l$, to increase critical spacing, if necessary.

As an example, consider the case where maximizing cam transmission ratio is of interest. To do so, one may either minimize the offset, $l$, or maximize the slot radius, $R$. Either choice essentially represents the same decision perEq. (3.14), so slot radius will be the focus here. Insight can be gained into the effect of increasing slot radius through Fig. 3.12 and Eq. (3.17). Using the triangle created between a arbitrary pin location on the path, the slot path center, and the center of cam rotation, the law of sines yields the relation given in Eq. (3.17).

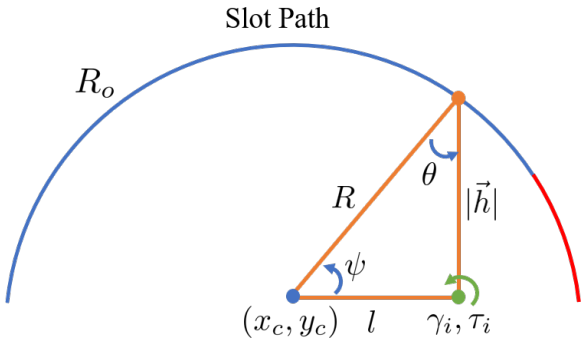


**Figure 3.12:** Analysis on the effect of increasing path radius (or reducing path center offset).

$$sin(\theta) = \frac{lsin(\psi)}{|\vec{h}|} \tag{3.17}$$

By increasing path radius (or reducing path offset), the sine of the critical angle, $\theta$, is minimized over the entire slot path. Furthermore, the magnitude of the vector connecting the cam center of rotation to the path, $|\vec{h}|$, increases for much of the path. Because the transmission ratio formula given by Eq. (3.11) is increased by reducing $sin(\theta)/cos(\theta)$ and $sin(\theta)$ is inversely proportional to $|\vec{h}|$, the transmission ratio can be increased by increasing $R$. Notably, greater transmission ratios are developed earlier in the path. As evidence, the

transmission ratio for a 17% increase in slot radius is presented alongside the original ratio development in Fig. 3.13.

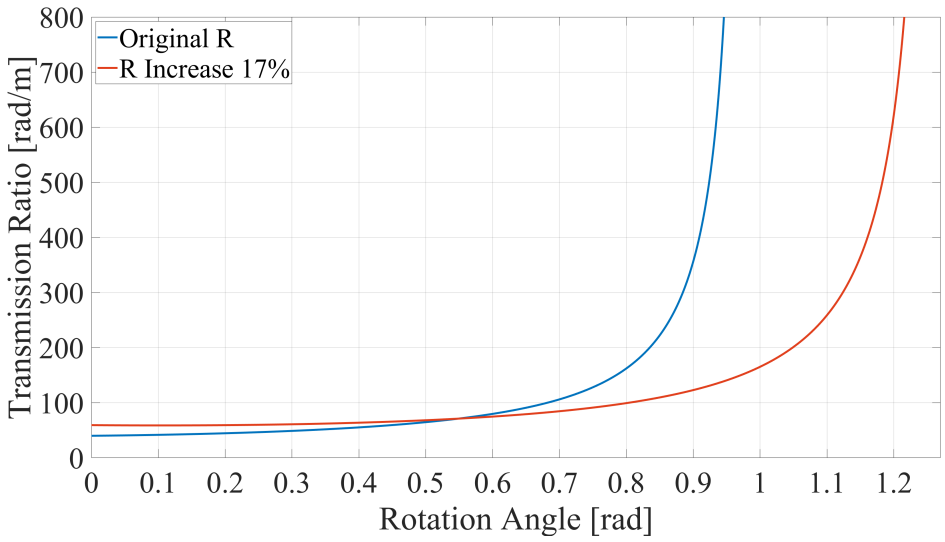


**Figure 3.13:** Increased slot radius in the spiral cam develops greater early-path transmission ratios.

Although the change in the transmission ratio profile shown in Fig. 3.13 appears to be modest or even detrimental in some cases (i.e., if deployment speed is more critical), in others it may be necessary. A case in point occurs when the grippers contact the terrain early in the rotation. If further gripper extension is required after contact, the mechanism must physically lift the weight of the vehicle imposed on the installation wheel. For instance, the prototype cam (see section 3.1) starts to lift the vehicle at 0.2775 radians of mechanism rotation (see Fig. 4.5). A further 0.7051 radians of rotation is required to fully expand the terrain grippers if it is conservatively assumed that the spikes produce no indentation into the terrain. At an arbitrary 0.2 radians of mechanism rotation, with $R$ increased as shown in Fig. 3.13, the cam offers a roughly 33% greater transmission than the original profile. This extra increase in transmission ratio allows the use of a smaller actuator. This is important when actuator size is severely constrained by the size of the mechanism.

# CHAPTER 4

# ELECTROMECHANICAL PROTOTYPE

Based on the analysis in Section 3, two adaptive wheel prototypes were created for use with the Georgia Tech AutoRally vehicle. The inner facing side of the prototype is shown in Fig. 4.1. A single prototype installs onto each of the AutoRally's rear, driving wheels. Each prototype features wireless communication and battery power and is easily mounted to the AutoRally wheels without additional wiring. The following sections describe the electromechanical design and fabrication of the system and the general method of installation on an existing vehicle like the AutoRally vehicle.

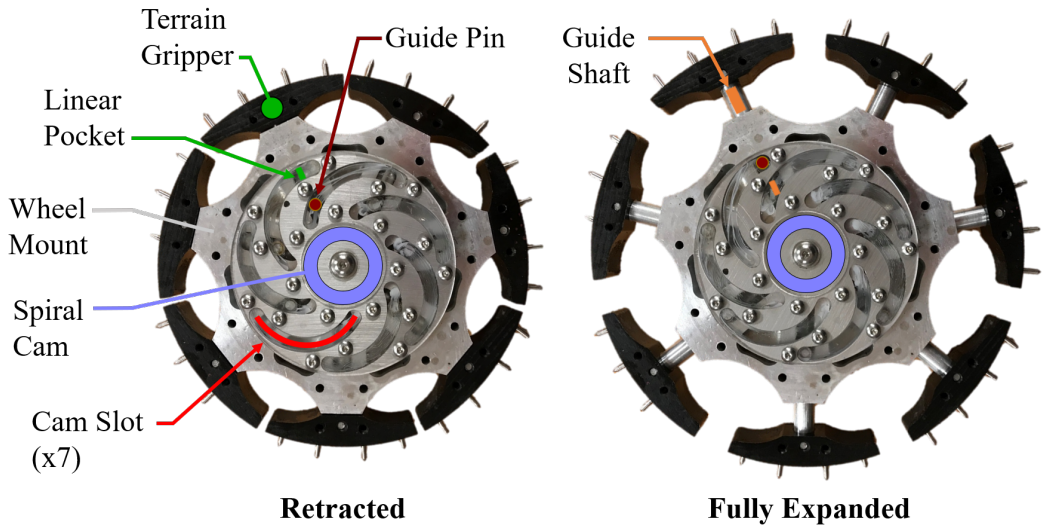


**Figure 4.1:** Annotated view of the mechanism prototype's inner facing side in its retracted and extended states.

## 4.1 Wheel Mounting

The adaptive wheel system can be thought of as beginning with the wheel mount, which fastens rigidly to the wheel's rim structure. Often, this connection requires the use of a simple adapter component, or "wheel mount adapter", like that shown in Fig. 4.2. As illustrated in Fig. 4.2, the inner face of the adapter mounts to existing features on a wheel rim. Such features may vary from vehicle to vehicle. For the GT Rally Vehicle, a series of existing thru-holes were modified to accommodate ten #8-32 screws used to connect the adapter and Nylon rim. The external face of the adapter contains a series of #6-32 threaded holes for the wheel mount to fasten to. For most kinematic and static analysis, the wheel mount may thus be considered as "fixed".

External mounting offers several advantages with regard to fitment with existing vehicles. The primary advantage is that it reduces conflict between the terrain grippers and existing vehicle features like the body, wheel well, suspension, or brakes. This is important because the grippers slightly increase the working diameter of the wheel at full expansion to ensure full gripper/terrain contact. By mounting externally, diametrical expansion exclusively occurs outside of existing vehicle features. The situation is further improved when the wheel structure features a large negative offset, as exemplified by Fig. 4.3. Here, offset defines the distance between: 1) the location of the wheel/hub connection and, 2) the plane that is both perpendicular to the wheel's axis of rotation and intersects the wheel center and. Although not strictly required for compatibility, negative offset causes the wheel to partially exist outside the wheel well. Fig. 4.3 demonstrates how the mechanism can mount to an existing vehicle.

Note that external mounting increases the vehicle's stance width slightly. For example, installation on the GT AutoRally Vehicle produced a stance width increase of 26.5%. Better resistance to tipping during aggressive turns is anticipated from greater stance width but is slightly offset by the increase in stance height created by the expanded grippers.

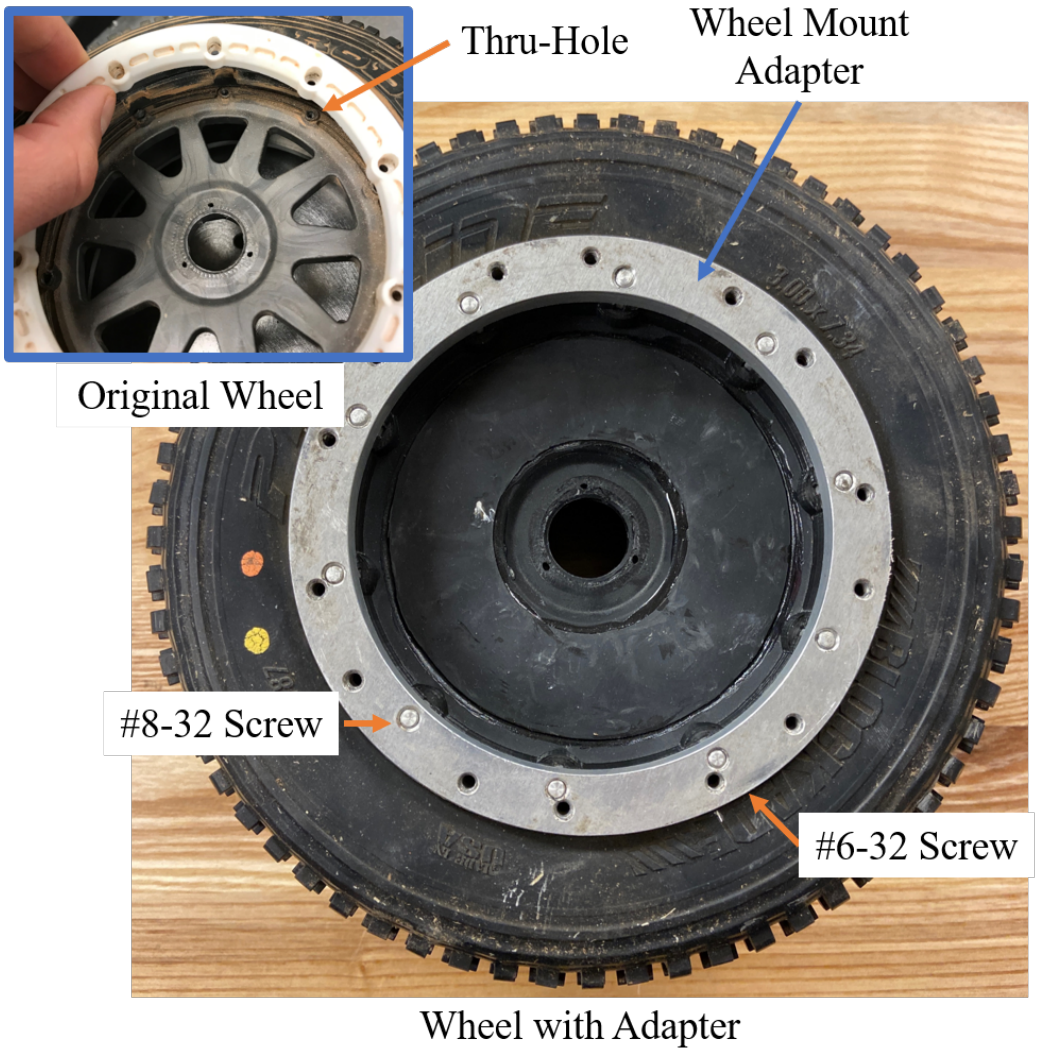


**Figure 4.2:** Illustration of the wheel mount adapter used to connect the adaptive wheel prototype to the stock wheels of the Georgia Tech AutoRally vehicle.

Observations from full-scale, however, suggest little change in turning performance.

An attractive feature of this mounting scheme is its compatibility with off-road-configured vehicles. For instance, trucks are commonly equipped with rims that feature a series of circumferential holes like that shown in Fig. 4.4. While such holes are commonly cosmetic in the stock configuration, often, they can be modified to support wheel loads with limited effort. This was the case in mounting to the AutoRally vehicle. Circumferential holes in the rim originally designed to mount non-structural components were drilled to accommodate mounting screws for the mechanism. If this is not possible, the lug bolts at the wheel/hub


**Figure 4.3:** Adaptive wheel system installed on an existing vehicle, demonstrating how negative offset allows the adaptive wheel mechanism to expand without interfering with existing vehicle features.

connection offers another feasible mounting location.

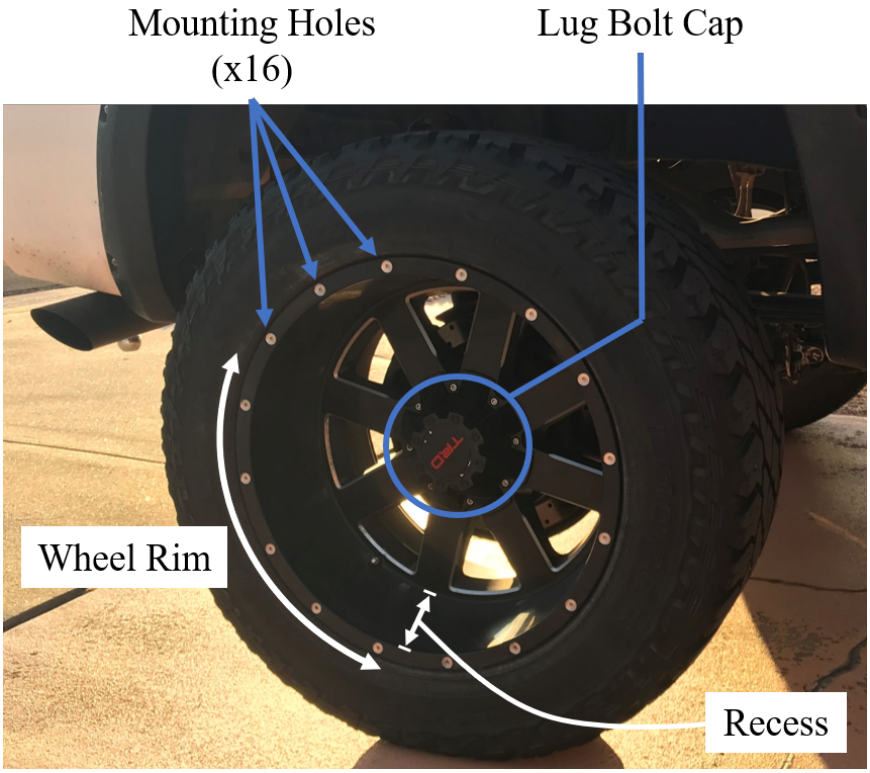


**Figure 4.4:** Example off-road truck wheel featuring a series of potential mounting holes.

## 4.2 Spiral Cam and Mechanism Actuation

The main function of the spiral cam is to convert input actuator effort to output movement of the terrain grippers. Based on the analysis presented in section 3.2, the cam acts as a variable gear whose transmission ratio derives from the geometric properties of its slots. Important design parameters for the prototype's circular cam slots are displayed in Table 4.1.

**Table 4.1:** Table of key spiral cam geometric properties utilized in the 3rd generation prototype.

| Variable | Value | Units | Description |
|---|---|---|---|
| $x_c$ | -1.900 | [cm] | Path offset (x-component) |
| $y_c$ | 0.000 | [cm] | Path offset (y-component) |
| $R$ | 2.388 | [cm] | Path radius |
| $d_o$ | 8.573 | [cm] | Maximum outer diameter constraint |
| $d_i$ | 5.690 | [cm] | Minimum inner diameter constraint |
| $t$ | 0.5 | [cm] | Cam thickness |
| $c$ | 0.4 | [cm] | Critical spacing between cam slots |

FEM analysis suggested that the prototype cam can safely support 54 Newtons of vehicle weight when a static *shock* loading factor of 5x is applied, or a total of 270 Newtons. The resulting factor of safety is greater than 2.0. The cam was manufactured using CNC and EDM techniques and is made of 6061-T6 aluminum. It is important to point out that the thickness of the cam is determined almost exclusively through the height of the friction reducing component used to interface between the guide pins and the cam slots. That is, maintaining adequate cam strength is done at minimal thickness, even with a cam produced from 6061-T6. This precluded the use of materials that exhibit greater strength/weight ratios.

To function optimally, frictional losses at all contacting interfaces must be minimized. There are three key interfaces: 1) slot/guide pin, 2) guide pin/linear pocket, and 3) guide shaft/wheel mount. Friction is minimized by utilizing both lubricated bushings and bal-

l/roller bearings. Installed at the top of each guide pin (i.e., location #1) is a lubricated bronze bushing that rolls along the inner contacting face of its cam slot. While better frictional performance results from a ball or roller bearing at this location, a bushing offers better shock resistance in a smaller package. Minimizing the size of the friction-reducing component allowed the use of a greater slot radius while maintaining a safe critical spacing.

The base of each guide pin presses into its respective guide shaft. During cam rotation, the guide pin base is forced into contact with pockets in the wheel mount to linearly constrain gripper expansion/retraction. At this interface (location #2), a ball bearing was pressed onto the guide pin. As a result, the outer diameter of the bearing rolls along the face of its linear pocket during gripper movements. At location #3, a tight-tolerance rotary bushing was used as a linear bearing to react transverse loads acting on the terrain gripper. This largely protects the ball bearing at location #2 during operation. Use of a rotary bushing instead of a linear bearing represented a trade-off between geometry and performance. To minimize the mass of the wheel mount (that houses the bearing), relatively little space could be allotted to the bearing. In this application, traditional linear bearings provide better frictional performance than rotary bearings but could not be reasonably accommodated due to spatial restrictions. A rotary bearing, however, provides reasonable linear frictional performance as long as it is kept well lubricated (boundary lubrication is stable). A high viscosity grease was used for this purpose due to the low stroke-velocity of the guide shaft during operation.

A pair of continuous-motion, Hitec HS-7245MH servo motors control deployment for each wheel mounted system. To amplify torque, a worm gear provides a 20:1 reduction between the motors' combined output and the spiral cam. The worm gear was selected because it provides relatively high torque amplification in a small package. Additionally, its housing can be made simple. A high viscosity grease lubricates the gears and is easy to seal in comparison to a gearing scheme utilizing free-flowing transmission oil or grease.

A keyed, $\varnothing 0.375$ inch central drive shaft transfers power from the output worm gear

to the spiral cam. The spiral cam is thereby constrained axially and radially and rotates concentrically relative to the wheel mount (and the wheel). Using the analysis in section 3.2, the required actuator torque can be easily calculated for the frictionless case. Of particular interest is the torque required when the terrain gripper begins to extend beyond the diameter of its installation wheel. This point is termed "vehicle pick-up" and represents the minimum required actuator torque. As shown in Fig. 4.5, the prototype's combined transmission ratio allows usage of a relatively low-torque actuator, even when anticipated friction is included. The roughly 1 kg-cm of required torque at vehicle pick-up can be compared to the combined 12.8 kg-cm of stall torque provided by the Hitec HS-7245MH servo motors used in the prototype.

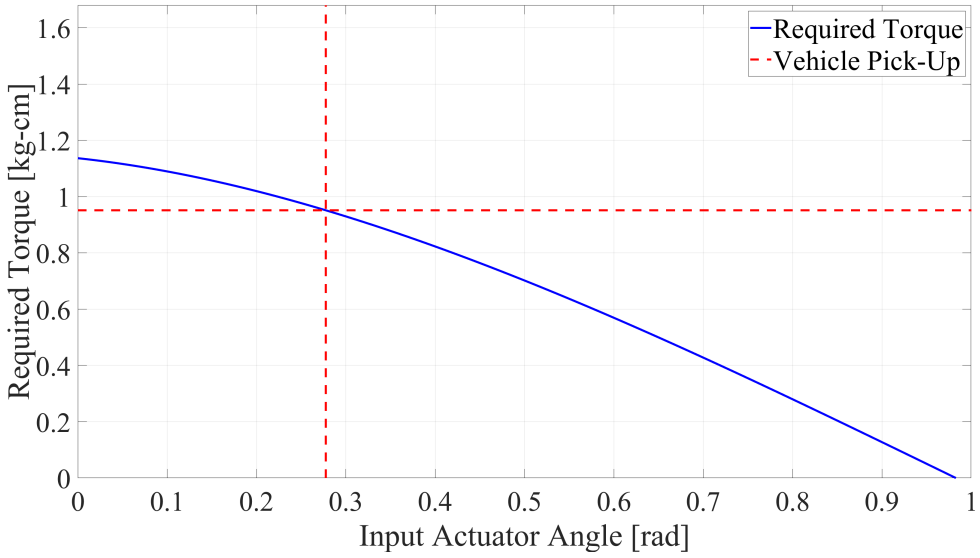


**Figure 4.5:** Actuator torque required to lift the 54 Newton, per-wheel AutoRally vehicle weight.

## 4.3 Terrain Gripper

Each terrain gripper interfaces with the spiral cam via its guide pin. The guide shaft links the the gripper base to the guide pin. It also bears operational loads when the gripper is fully extended and in contact with the terrain. Design loads consist mainly of axial and bending

types. In the extended configuration, axial loads are transferred directly through the gripper base and guide shaft and terminate at the interface between the guide pin and spiral cam slot. This imposes significant bending stress on the guide pin. It is conservatively assumed that a single guide pin must react the full axial load. Consequently, the guide pin is made from a through-hardened steel dowel pin and rigidly connects to its guide shaft via a light press fit. In this work, a $\varnothing 3/16$ dowel pin was used.

Moments deriving from wheel torque or vehicle maneuvering are reacted through the wheel mount via a 0.75-inch long bronze linear bearing. To minimize weight and maximize strength, the $\varnothing 0.375$ inch guide shafts were made of 7075-T6 aluminum, which is extensively used in structural aircraft parts. At full extension, the gripper base extends 0.5675 inches radially from its fully-retracted position in the wheel mount.

On the outer face of the gripper is an annular section with a series of blind holes machined into its surface. To create a high friction surface, components can be mounted to these blind holes. This work utilizes sharpened, $\varnothing 3$ mm steel dowel pins, as shown previously in Fig. 3.7. The hardened steel dowel pins are affixed to each blind hole with a pressed-on plastic sleeve. Before installation, the pins are sharpened to a point and are intended to remain sharp during operation of the mechanism.

As discussed later, the sharpened dowel provides adequate terrain indentation but is particularly prone to failure in bending. To alleviate the bending issue, a 2nd-generation gripper prototype was created (but not tested) and is shown in Fig. 4.6. Using conical grippers, as opposed to sharpened dowel pins, is particularly suited to hard terrain like ice because the expanded base provides better resistance to bending moments.

## 4.4 Electronics and Control

The adaptive wheel system is designed for wireless control and independent power. The on-board electronics are housed in two separate mechanism components: the wheel mount and the hub cap. The wheel mount, in additional to housing power and a portion of the


**Figure 4.6:** Alternative terrain gripper designs, like that shown with a conical spike, can provide improved performance on relatively hard terrain like ice.

electronics, also houses the actuators. A photograph of the wheel mount's electromechanical components is provided in Fig. 4.7. All associated components are housed with a sealed recess in the wheel hub, which is located on the side opposite the spiral cam. This recess contains a lithium-polymer (Lipo) battery (2S, 750 mAh), the two aforementioned Hitec HS-7245MH servo motors, two motors drivers, a Hall effect sensor, a power switch, and a momentary to latching switch converter. Note that two motors simultaneously drive the worm and gear, the latter of which are centrally located in Fig. 4.7. The gear then rotates with the spiral cam.

The hub cap houses the microcontroller unit (MCU), a simple voltage divider, and an Xbee radio, as shown in Fig. 4.8. Computational requirements are kept extremely low in this setup such that an Arduino Pro Mini with a 5V/16MHz ATmega328 MCU provides ample performance. The voltage divider is used as a simple monitor for the battery voltage. More accurate setups may benefit from more sophisticated batter management systems. An Xbee Pro S2 radio module provides wireless communication with an external device: in this case, a laptop with another Xbee radio module. Custom printed circuit boards (PCBs) were manufactured to organize the electronics in both the wheel mount and hub cap.

Each adaptive wheel system is controlled using wireless signals sent to the Xbee radio transceiver. A simple bang-bang control scheme commands the motors either full forward,

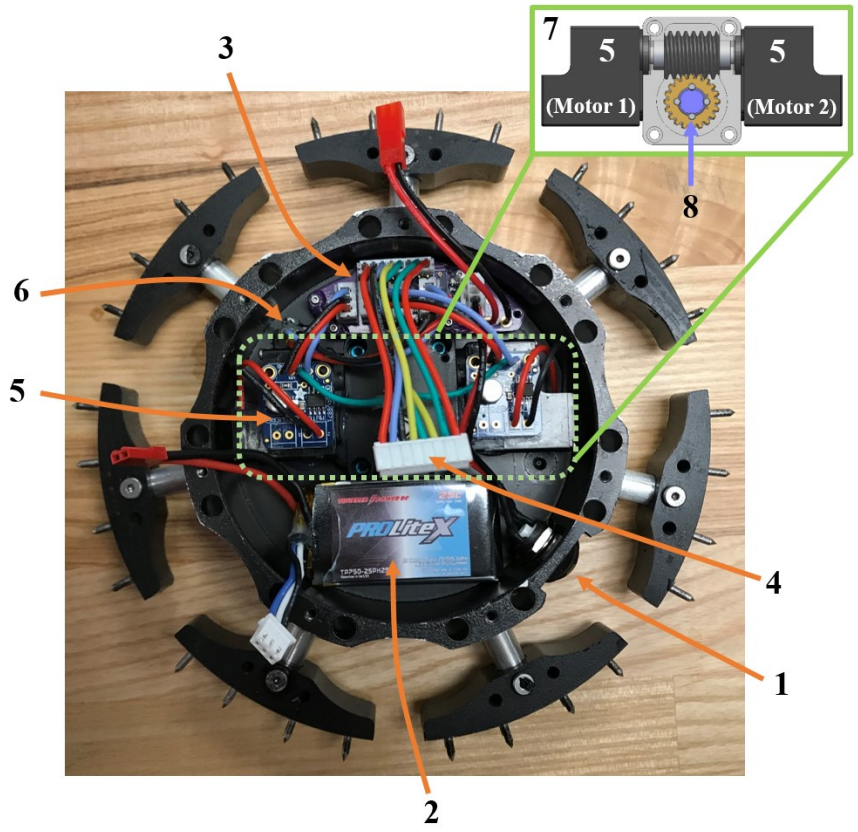


**Figure 4.7:** Annotated power motherboard photo: 1. Power switch, 2. 750 mAh, 2S Lipo, 3. Wheel mount motherboard, 4. Connection to MCU motherboard, 5. Hitec HS-7245MH servo motor and driver, 6. Hall effect sensor, 7. Power train with worm, gear, and motors, 8. Central drive shaft (to spiral cam).

full reverse, or halted. Stemming from the binary operation of the mechanism (either retracted or expanded), the bang-bang control scheme was deemed appropriate. Due to this control, efforts were not explicitly made to minimize gear backlash. The Hall effect sensor is installed into the hub and senses magnets affixed to one of the mechanism's guide shafts. Feedback from the Hall effect sensor is used to terminate motions at either end of travel. For reference, mechanism state changes occur in roughly 2 seconds and draw an average of 1 amp. When the motor is not utilized, the system draws roughly 50 mA. While endurance depends on use scenarios, if the system is switching continuously, each wheel can, in theory, change state up to 1240 times before a battery recharge is needed.

The system has been designed for an IP68 rating. This enables full liquid submersion.

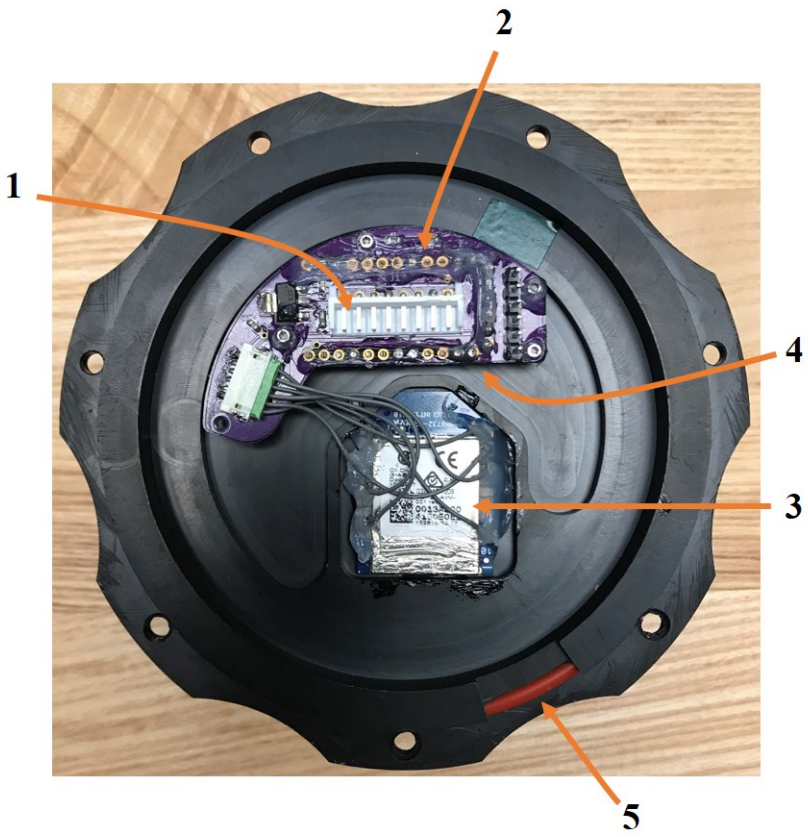


**Figure 4.8:** Annotated MCU motherboard photo: 1. Connection to power motherboard, 2. Battery voltage monitor circuit, 3. XBee-PRO radio module, 4. (Under circuit board) Arduino Pro Mini MCU, 5. O-Ring seal.

The mechanism cap achieves this with an O-ring during attachment to the hub. All other ports in the mechanism are either potted or have their own O-ring for sealing. In total, each mechanism adds approximately 1.18 kg to a wheel. In relation to the original GT AutoRally vehicle, installation of two mechanisms increases the total vehicle weight by approximately 11%. It is anticipated that this weight penalty can be reduced through further optimization of geometry, material selection, and manufacturing methods.

# CHAPTER 5
# PERFORMANCE QUANTIFICATION

## 5.1 Terrain Gripper Testing

To quantify the performance of the terrain grippers relative to the original tire, a simple test cart, shown in Fig. 5.1, was employed in a series of static friction tests. These tests measured holding force at the onset of motion.

Compatibility with the test cart required the creation of modified terrain grippers. Four such grippers attach to the base of the cart and bear close resemblance to those installed on the actual mechanism. The difference is that modifications to the implementable gripper design were made for installation on the test cart. For instance, the rubber tire test grippers utilize a 3D-printed plastic arc with a diameter equal to that of the original tire. Sections were cut from an AutoRally car tire and glued to these plastic arcs to form the test grippers. With respect to an actual tire, the plastic arc alone would simulate an artificially rigid tire foam core, as the AutoRally tire utilizes a foam interior. Consequently, reported friction from this gripper construction would be expected to exhibit lower baseline friction values due to the general frictional enhancement tires exhibit at lower tire pressures (for a pneumatic tire) or stiffnesses (for a tire with a foam core). This was mentioned in section 3.1.3. To more realistically simulate tire compliance, a section of polyurethane foam was glued between the plastic arc and rubber tire strip. Provisions of this nature were not required for the sharp and blunt spike test grippers.

With the grippers installed, the cart was then positioned on a flat section of terrain, loaded with weight, and pulled parallel to the terrain with a precision spring force gauge. Once motion began, the experiment was stopped and the peak holding force recorded. Peak holding force was verified via 60 fps video analysis and recorded for a set of cart weights

**Figure 5.1:** Traction cart used to measure gripper static friction.

ranging from 5.4 to 43 Newtons. A measure of static friction was determined by fitting a line to the *holding force versus normal force* data.

Measurement accuracy is an important consideration during testing, of which two general types were present: component accuracy (force gauge) and measurement variability (test conditions versus assumed). Component-wise, the force gauge specifies a reading accuracy of $\pm 25$ grams. Converted to newtons, the maximum expected accuracy over the range of test weights varies from 0.5% to 4.6%. Based on the variability in test conditions, namely surface conditions (i.e., planar, horizontal nature) and gauge pull force trajectory (degree of actual surface/pull parallelism), the actual accuracy is expected to be lower but is not provided here. The intent of such testing is to measure the relative traction afforded by each gripping device. It is not meant to extract universal coefficients of static friction.

A minimum of four experiments were performed for each test weight. The results are shown in Figs. 5.2 to 5.4. Each data point represents the mean slip force and the associated standard deviation at each test weight. The lines represent the least-squares linear fit to the data. In general, the observed standard deviations fall within 20%. Twenty percent deviation was deemed an acceptable upper bound due to the relatively large differences in slip force between the grippers.

As can be seen, the sharp spike grippers produce significantly more static friction than

the rubber tire and a blunt spike designs. If the AutoRally vehicle's per-wheel weight of 54 N is substituted into a linear model of the data, the spiked gripper's traction relative to the rubber tire is roughly 160% greater on dry packed dirt, 190% greater on grass, and 320% on greater ice. Dynamic friction testing is expected to produce similar trends, albeit at lower absolute friction values. In light of this work's goal to ensure friction remains, dynamic friction testing was not conducted.

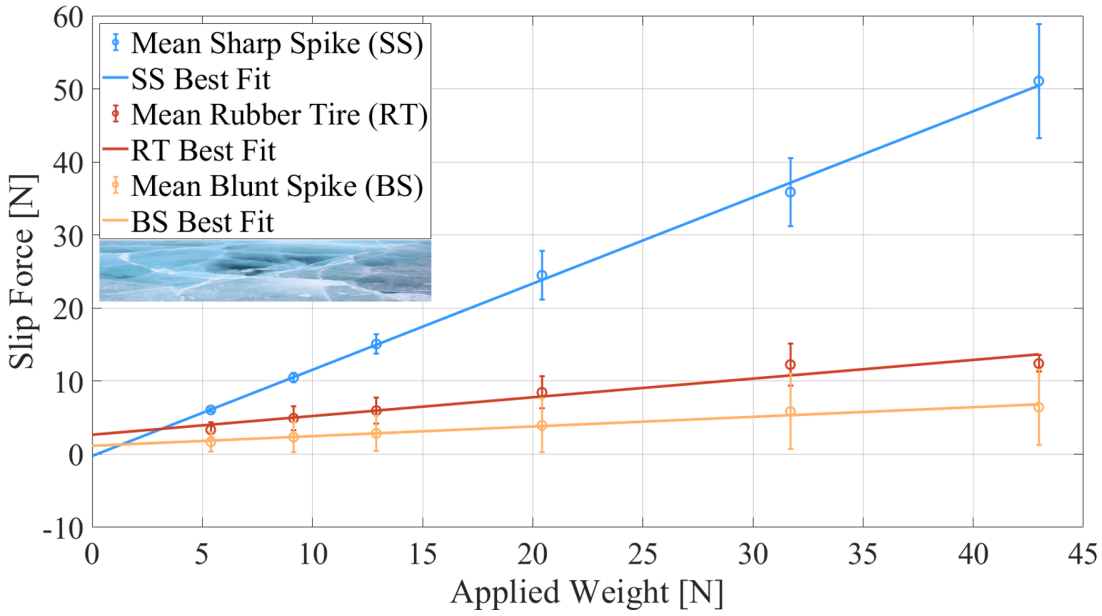


**Figure 5.2:** Slip force versus normal weight for various terrain grippers on ice.

Blunt spikes were included in these plots to demonstrate the importance of creating and maintaining indentation (via a sharp point) with the terrain gripper design. This is illustrated in Fig. 5.2, where the blunt spike under-performs the tire by approximately 85% over the range of test weights. It is clear that the blunted spike produces little appreciable surface gouging. The remaining frictional mechanism is adhesion, which does not provide sufficient friction on relatively hard surfaces in this configuration. Note, however, that on the softer dirt and grass terrains, the blunt spike's performance mimics that of the sharp spike.

The blunt spike's poor performance on ice helps underscore the need for controllable deployment and the merit of a modular gripper design. Hard, abrasive surfaces like dry

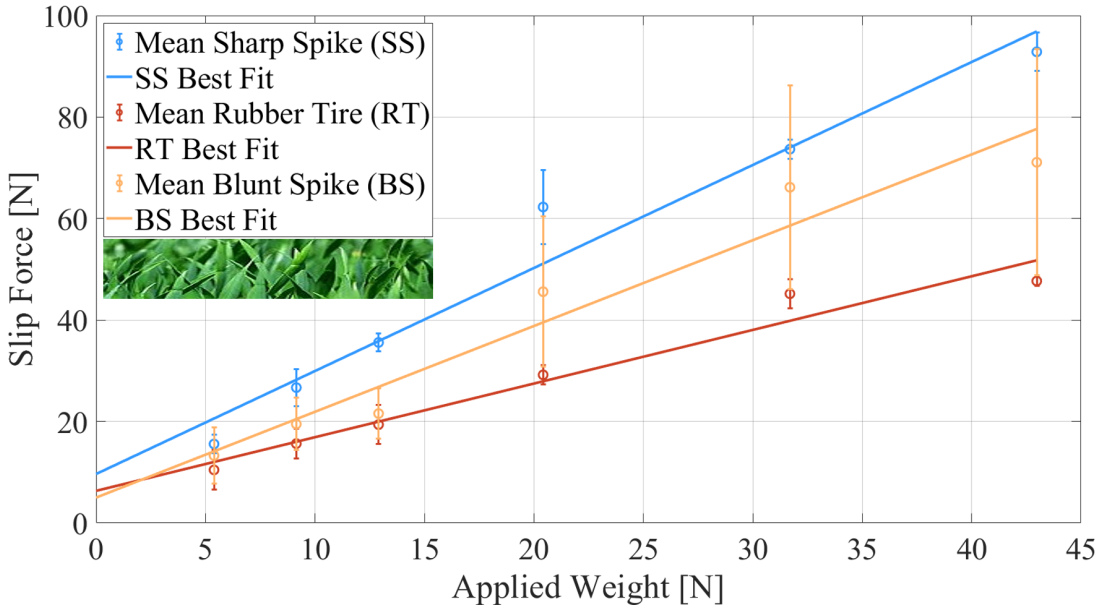


**Figure 5.3:** Slip force versus normal weight for various terrain grippers on grass.

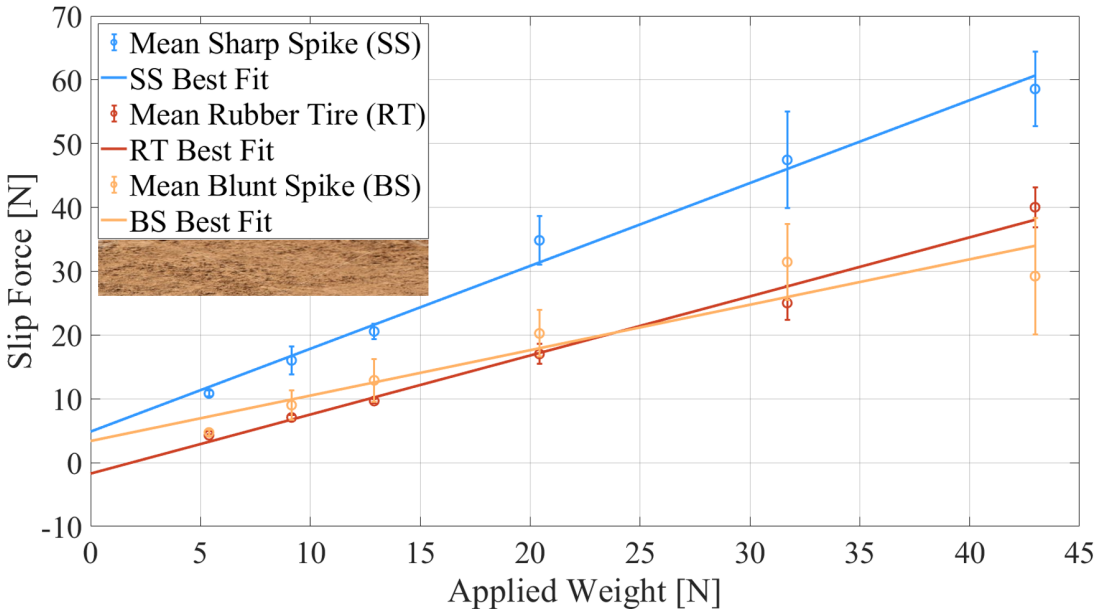


**Figure 5.4:** Slip force versus normal weight for various terrain grippers on dry, packed dirt.

asphalt are liable to produce accelerated wear on rigid gripping elements like spikes and are much more suitable to the tire's use. Gripper control allows retraction on such surfaces to promote long-term indentation on more suitable surfaces and maximize vehicle performance. Control, however, does not completely obviate accidental deployment risks. There

is a marked need to monitor the condition of the spikes to ensure optimal performance. Long-term testing will confirm the longevity of the steel spike design under such conditions, but since the grippers are easily replaced, performance losses from blunted spikes can be readily restored by installing new grippers.

That said, steel spikes arranged into symmetric arcs may not provide optimal, sustained performance. If better wear performance is required, a first step may be to manufacture the gripper spikes from harder or stronger materials than hardened steel such as carbide. This essentially mimics the approach taken by the metals manufacturing industry through the introduction of carbide tooling. Another option is to increase the number of spikes per gripper such that blunting events (i.e., impact with hard or unintended terrain like asphalt) impact a smaller percentage of spikes. Alternatively, the grippers may be arranged into patterns that produce more uniform wear. Efforts of this nature are reserved for future work.

The dramatic frictional increases demonstrated by the grippers' sharp-spike approach suggest similar gains in full-scale testing. However, lower relative frictional performance was observed due to gross slippage of the grippers, among other factors. Full-scale test results are the topic of section 5.3.

## 5.2 Spiral Cam Transmission Ratio

Kinematic experiments were performed to validate the spiral cam design model developed in section 3. Using a standard 60 fps video recorder, two different, high-visibility paints of different color were applied to the spiral cam and a single gripper. A recording of the mechanism was then taken as the mechanism was hand-actuated. Color tracking software logged the position of each marked component as a function of time. Gripper position versus actuator rotation data was then compared to that predicted by the spiral cam model. The results are shown in Fig. 5.5.

As can be seen from Fig. 5.5, the transmission behaves as predicted. Radial velocity of

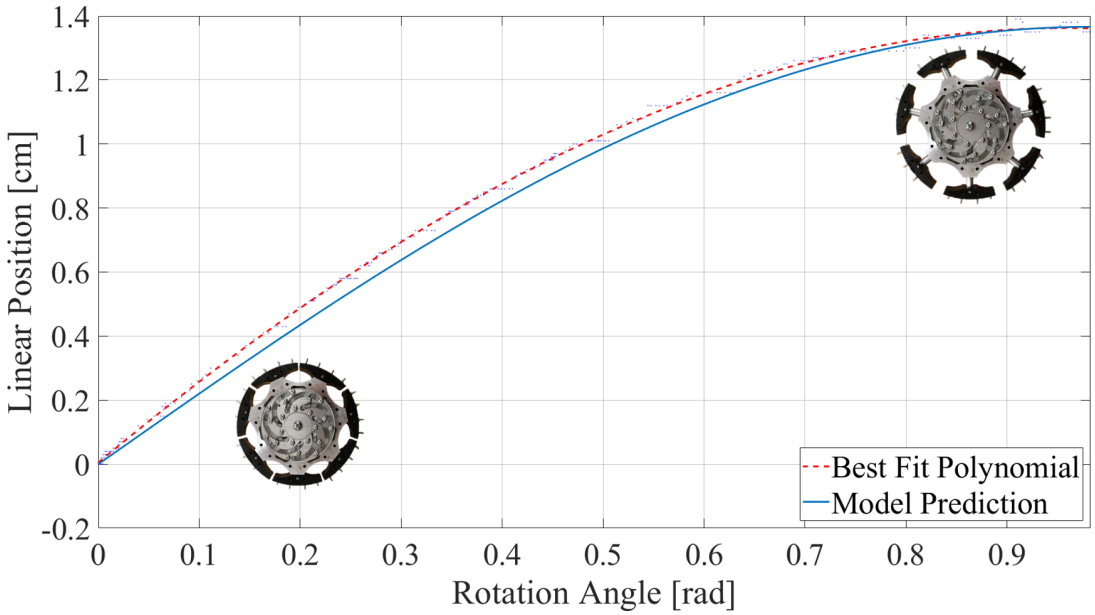


**Figure 5.5:** Modeled output of the spiral cam versus the measured response.

the gripper is greatest at the start of its stroke (from a retracted state) and gradually evolves toward zero at the end of its stroke (grippers fully expanded). This exhibits a suitable balance between gripper deployment speed, actuator torque requirements, and development of a singular configuration at end-of-stroke. A natural advantage of the spiral cam is thus the ability to predictably shape its transmission ratio through geometric manipulation of its slots, as described previously.

Being a kinematic measure, the results in Fig. 5.5 obscure the detrimental effects arising from frictional losses in the mechanism. The importance of minimizing frictional losses cannot be understated. An early prototype notably overlooked this necessity. The guide pins were allowed to slide along their cam slot and linear pocket interfaces, which resulted in extremely poor torque transmission. In some cases, the mechanism become completely inoperable because of frictional losses. In the current prototype, however, the use of bushings and ball bearings reduce losses to less than 10%. If ball or roller bearings are exclusively employed throughout, losses of less than 1% are anticipated.

## 5.3 Deployment Testing

Full system performance was evaluated by installing an adaptive-wheel mechanism on each of the rear (driving) wheels of the Georgia Tech AutoRally platform [5]. The AutoRally platform consists of a modified HPI Baja 5SC 1:5 scale rally car and an on-board computing and sensing system. The system weighs roughly 220 Newtons and has a top speed of 90 km/h. The car uses a rear-wheel drive system that is actuated by a 10-hp electric motor; power draws from a pair of 4S, 14.8 V lithium-polymer batteries connected in series. For full details on the AutoRally platform, the reader is referred to [5].

Based on the terrain gripper traction results presented in section 5.1, quantitative performance testing of the sharpened spike design was conducted on ice and dirt. To simulate ice, PolyGlide synthetic ice sheets were rigidly fastened to a $1.25\,\mathrm{m} \times 2.5\,\mathrm{m}$ wooden platform. The synthetic ice covered all but the platform edges. The platform was then anchored into the ground via spikes at each of the four platform corners to ensure a rigid connection with the ground. To simulate the effect of water bleed on natural ice, the synthetic ice was also wetted before each trial.

An acceleration test was used to quantify performance. Ice trials began with the vehicle positioned at one end of the platform. A step input command was then the sent to the motor controller on board the vehicle. Each trial concluded once the front tires reached the edge of the platform, constituting a total travel distance of approximately 1.5 meters. Dirt trials were conducted in the same manner but on a dirt track used by the Georgia Tech AutoRally group.

All trials were conducted with the mechanism installed and with the step input command set to 70% of full throttle. The baseline case held the terrain grippers retracted so that only the rubber tires made contact with the terrain. Test trials were then conducted with the grippers extended to fully contact the terrain. Video analysis akin to that used in validating the spiral cam was employed to measure the kinematics of the vehicle during each trial. To

track motion, a high-visibility pink dot was painted on the side of the vehicle's body at the approximate center of mass. The results are shown in Fig. 5.6. Video was recorded at 60 fps with a wide lens angle mounted perpendicular to the vehicle's motion. Two trials were conducted for each terrain/configuration.

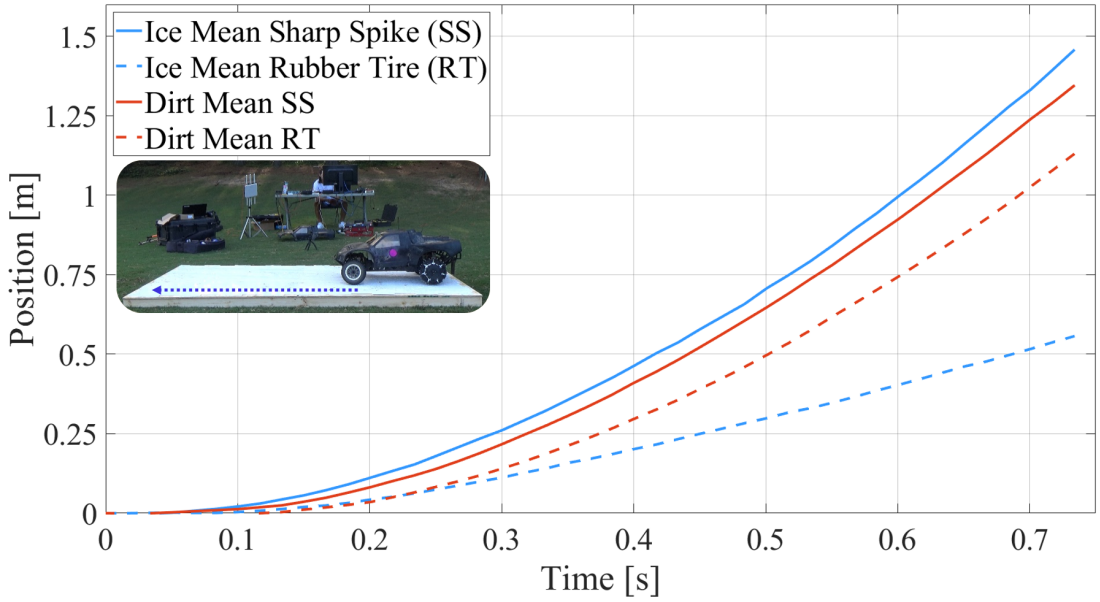


**Figure 5.6:** Synthetic ice and dirt trial results with and without grippers deployed on the Georgia Tech AutoRally vehicle.

From the position profiles shown in Fig. 5.6, the advantage of the terrain gripper is evident. When an acceleration coefficient is fitted to the data, the resulting value is 171% greater on ice and 14% greater on dirt with the grippers engaged than with the original rubber tire. The modest gain on dirt is attributed to unusually good rubber traction on the wet, clay-heavy trial dirt tested on. Results on dry dirt and grass are expected to follow trends similar to those observed from static terrain gripper testing.

The terrain gripper, as designed, demonstrates promise for particularly challenging terrain. However, lower relative gripper performance is seen in comparison to static friction testing. One source of this disparity is the incidence of gross slippage of the spikes during vehicle testing, which is visibly present in the video and introduces intermediate frictional values between that observed from the static cart tests and that deriving from pure kinetic

friction. Concurrently, friction is decidedly based on the rate of loading [54, 55]. Load rates during static testing were much lower than in full-scale testing and similarly suggest intermediate frictional regimes rather than the greater magnitude, static regime. Subsequently, comparison to the purely static cart test results is no longer appropriate. Nevertheless, the grippers were still able to offer a dramatic performance increase on the more challenging terrain (synthetic ice).

A significant part of the slippage issue derived from spike damage, and failure to prevent gross slippage represents inadequacy of the terrain grippers employed. This is particularly evident when considering that the terrain gripper spikes tended to sustain considerable damage during testing. Examination of the sharpened dowel pins post-testing revealed widespread damage: bent dowel pins, deformed dowel pin sleeves, or outright ejection of the dowel pins from the gripper. Damage was more pronounced following synthetic ice tests than after dirt tests. The nature of the damage points to failure in bending, which may be remedied by widening the diameter of the spike at its connection point to the gripper body. Alternatively, more spikes may be fixed to the gripper body to reduce the force burden. The nylon spike sleeve, originally intended to protect the gripper body from damage, also warrants reassessment. It may be replaced with a stronger material or altogether removed from the setup, as is the case for the threaded, conical gripper highlighted in Fig. 4.6.

To maximize performance with an adequate spike, updates to the current car controller are also required. Specifically, throttle values approaching 100% and inputs more closely resembling step inputs are of interest. The expected result is a further increase in loading rate beyond that achieved here. It is crucial, therefore, that the gripper maintain static hold on the terrain. In such cases, it may be necessary to reassess the indentation capability of the gripper spikes. Maximizing adaptive performance with control and gripper redesign is a topic for further study.

While the initial studies have focused on acceleration performance, turning and stop-

ping can also be affected by the adaptive mechanism. If the vehicle does not slip during a turn, no degradation in turning behavior is anticipated. However, at sufficient speeds, increased friction from deployed spikes may impact behavior. This can be positive (reducing lateral slip) or negative (tipping of the vehicle). Given its demonstrated benefit, it is expected that the deployed terrain grippers will improve stopping performance when brakes are used. The current AutoRally platform, however, does not utilize brakes and stops through a combination of light motor reversals and coasting.

# CHAPTER 6
# CONCLUSION

This paper presented the design, analysis, and implementation performance of a novel system for actively modulating vehicle traction. The functional requirements set forth for adaptive friction augmentation provided a basis for a new type of mechanism that is actuated through a unique spiral cam. The mechanism controllably deploys a series of terrain grippers to enhance friction on a set of target terrains common to off-road environments: hard-packed dirt, grass, and ice. The spiral cam serves as a compact rotary-linear transmission whose slot geometry can be tuned based on an application's unique requirements. Manipulation of such geometry allows the development of a singular configuration to minimize power consumption and enhance system robustness. Bench level experiments conducted illustrate frictional improvements and validate the intended transmission behavior. To assess implementable frictional performance, two prototypes were created. Integrated on a scaled vehicle, the mechanism demonstrates how friction modulation can greatly improve performance on challenging surfaces like artificial ice.

A primary system goal was modularity and robustness. However, notable design changes to the current prototype are required to maximize performance. In its current configuration, the spikes can rather easily deform (bend) or tear out of the terrain gripper. This is a result of attempts to make the design modular and to protect key components (i.e., the gripper body) from damage. However, relatively pronounced spike damage sustained during full-scale vehicle testing produced gross slippage and truncated frictional performance. Moreover, inadequate sealing at the gripper/wheel mount interface allowed unacceptable foreign matter ingress into key friction reducing components in the mechanism. These issues have been addressed, and methods for more permanent, robust installations are available for future testing.

The approach presented in this work is uniquely suited to existing, unmanned ground vehicles that must drive aggressively on a wide range of surfaces. Controllable deployment of the grippers expands the vehicle's traction performance to a greater set of terrains, as the grippers can be deployed on surfaces with demonstrated performance gains and retracted elsewhere to allow the original rubber tires to operate uninhibited. Compatibility with existing vehicles produces attractive use cases for broad deployment. Not only can the mechanism easily mount to the wheels of existing vehicles, integrated control is readily available through a simple wireless interface. These techniques, combined with ground property estimation and adaptive control, hold particular promise in achieving greatly enhanced autonomous driving performance.

# Appendices

# APPENDIX A

# MECHANISM CONTROL ROUTINE

The program used to control the friction-modulating mechanism is presented below. It was written in the Arduino environment and utilizing an Arduino Pro Mini development board featuring an 8-bit, AVR, 5V/16MHz atmega328p microcontroller. Utilizing interrupts to minimize electronic component power draw, the program monitors the battery voltage to assess charge, wirelessly communicates with a remote controller, actuates the two DC drive motors, and monitors terrain gripper position changes to assess their state of expansion (expanded or retracted).

```
/*  Function: ActiTrac On-Wheel Control
 *
 *
 *  Hardware:
 *  - Arduino Pro Mini 328 (atmega328p AVR MCU)
 *  - Pololu LV Mini Pushbutton Power Swtich
 *
 *  Bootloading MCU:
 *  1) Open Device Manager, open FTDI port advanced settings, select "
   RTS on close"
 *  2) Board: Arduino Pro or Pro Mini
 *  3) Processor: ATmega328P (5V, 16MHz)
 *
 *  Communication Protocol:
 *  1) All commands sent must end in a '.'
 *  2) 'expand.' expands the mechanism
 *  3) 'retract.' retracts the mechanism
 *  4) 'stop.' stops the current movement
 *  5) 'battery.' queries the battery charge status
```

```
 */
//
   ------------------------------------------------------------------------------


//-- Library Includes --//
#include <stdio.h>
#include <avr/io.h>
#include <avr/interrupt.h>
#include <avr/sleep.h>
#include <string.h>

//-- Defines --//
#define BUF_SIZE 35                // Receive buffer size
#define TIME_OUT 3000              // Expansion/retraction movement
   timeout (used as failsafe), in ms
#define F_MCU 16000000
#define USART_BAUDRATE 38400
#define UBRR_VALUE (((F_MCU / (USART_BAUDRATE * 16UL))) - 1)
#define timeOut_norm 2500
#define timeOut_fault 2500
#define bat_buf 10

#define HE1_PIN 2
#define HE2_PIN 3
#define MC1 6
#define MC2 11
#define OFF_PIN 12

//-- Global Variable Declaration --//
int timeNow, moveState = 0;                // Motor movement state (-1
   = expanding, 1 = retracting, 0 = stop)
volatile char readFlg = 0, motorFlg = 0, fault = 0, repFlg = 0;
```

```
48 volatile int counter = 0, HEcounter = 0;
49 volatile int timeOut = 0xFFFFFFFF;
50 char timeOutFlg, normFlg = 0;
51 char batStat[bat_buf];
52 char lastState[BUF_SIZE];
53
54 //-- RX/TX indices and buffers --//
55 typedef struct{
56     uint8_t Buffer[BUF_SIZE]; //Array of chars
57     uint8_t index;    // Rx array element index
58 }u8buf;
59 u8buf buf;  //declare buffer
60
61 //
    ------------------------------------------------------------------------------
62 void setup()
63 {
64   pinMode(HE1_PIN, INPUT);
65   pinMode(MC1, OUTPUT);
66   pinMode(MC2, OUTPUT);
67   pinMode(OFF_PIN, OUTPUT);
68   digitalWrite(OFF_PIN, LOW);
69
70   strcpy(lastState, "Retract.");
71
72   DDRD &= ~(1 << DDD2);     // PD2 (D2, PCINT0 pin) is now an input
73   EICRA |= (1 << ISC00);    // Set INT0 to trigger on ANY logic change
74   EIMSK |= (1 << INT0);     // Turns on INT0
75
76   Buffer_Init(&buf);               // Initialize buffer
77   set_sleep_mode(SLEEP_MODE_IDLE);  // Set sleep mode
78   USART0_Init();                   // Initialize USART0
```

```
79    sei();                              // Enable global interrupts
80  }
81
82  //
      ------------------------------------------------------------------------------
83  void loop()
84  {
85    motorControl();
86
87    while(readFlg == 0 && moveState == 0)
88    {
89        sleep_mode(); // Put MCU to sleep
90    }
91    if(readFlg == 1)
92    {
93      TX_WRITE(&buf);
94    }
95    else if(repFlg == 1 && UCSR0B == ~((1<<TXEN0)|(1<<UDRIE0)))
96    {
97      setRep(&buf);
98    }
99  }
100 //
      ------------------------------------------------------------------------------
101 //-------------------------
102 // Motor control routine
103 //-------------------------
104 void motorControl()
105 {
106   timeNow = millis();
107   // If motor times out before reaching end of stroke
```

```
108  if((timeNow - timeOut) >= timeOut_norm && counter == 1)
109  {
110    timeOutFlg = 1;
111  }
112  else if((timeNow - timeOut) >= timeOut_fault && counter > 5)
113  {
114    timeOutFlg = 1;
115  }
116
117  if(timeOutFlg == 0 && moveState != 0)
118  {
119    if(counter == 0)
120    {
121      counter = 1; HEcounter = 0; // Set HEcounter in case of MCU start
      up counting
122      timeOut = millis(); // If HE sensor fails to trigger on motor
     start
123    }
124    else if(counter == 5)
125    {
126      counter++; HEcounter = 0;
127      timeOut = millis(); // If motor starts and is mid stroke
128    }
129  }
130
131  if(motorFlg == 1 || timeOutFlg == 1) // Sets counter = 0 if motorFlg
      == 1
132  {
133    motorShutDown(&buf);
134  }
135
136  if(moveState > 0)
137  {
```

```
138     digitalWrite(MC1, HIGH);
139   }
140   else if(moveState < 0)
141   {
142     digitalWrite(MC2, HIGH);
143   }
144   else
145   {
146     digitalWrite(MC1, LOW);
147     digitalWrite(MC2, LOW);
148   }
149 
150   delayM(5); // Delay 5 milliseconds
151 }
152 //-------------------------
153 // Set repeat
154 //-------------------------
155 void setRep(u8buf *buf)
156 {
157   memset(buf->Buffer, '\0', BUF_SIZE);
158   strcpy(buf->Buffer, lastState);
159   repFlg = 0;
160 }
161 //-------------------------
162 // Motor control routine
163 //-------------------------
164 void motorShutDown(u8buf *buf)
165 {
166   if(timeOutFlg == 1)
167   {
168     char TX_SEND[] = "Movement Timeout: Stopping...\r\n";
169     memset(buf->Buffer, '\0', BUF_SIZE);
170     strcpy(buf->Buffer, TX_SEND);
```

```
171
172     UCSR0B &= ~((1<<RXEN0)|(1<<RXCIE0));  // Disable reception and RX
        Complete interrupt
173     UDR0 = buf->Buffer[buf->index];       // Initiate transfer
174     UCSR0B |= (1<<TXEN0)|(1<<UDRIE0);     // Enable transmission and
        UDR0 empty interrupt
175     counter = 5; fault = 1;
176   }
177   else if(motorFlg == 1)
178   {
179     HEcounter = 0, counter = 0;
180   }
181   if(moveState == -1)
182   {
183     delayM(750); // Delay
184   }
185   else if(moveState == 1)
186   {
187     delayM(275); // Delay
188   }
189   moveState = 0, timeOutFlg = 0, motorFlg = 0;
190 }
191 //-------------------------
192 // Hall effect sensor #1 ISR
193 //-------------------------
194 ISR (INT0_vect)
195 {
196   HEcounter++;
197   if(HEcounter > 1)
198   {
199     motorFlg = 1;
200   }
201 }
```

```
202 //-------------------------
203 // RX send confirmation routine
204 //-------------------------
205 void TX_WRITE(u8buf *buf)
206 {
207   buf->index = 0;
208   char TX_SEND[BUF_SIZE];
209 
210   if(strcmp(buf->Buffer,lastState) == 0 && strcmp(buf->Buffer,"stop.")
       != 0)
211   {
212     strcpy(TX_SEND,"Repeated command. Resend...\r\n");
213     repFlg = 1;
214   }
215   else if(strcmp(buf->Buffer,"expand.") == 0)
216   {
217     moveState = -1;
218     strcpy(TX_SEND,"Expanding...\r\n");
219     memset(lastState, '\0',BUF_SIZE);
220     strcpy(lastState,"expand.");
221   }
222   else if(strcmp(buf->Buffer,"retract.") == 0)
223   {
224     moveState = 1;
225     strcpy(TX_SEND,"Retracting...\r\n");
226     memset(lastState, '\0',BUF_SIZE);
227     strcpy(lastState,"retract.");
228   }
229   else if(strcmp(buf->Buffer,"stop.") == 0)
230   {
231     motorFlg = 1;
232     strcpy(TX_SEND,"Stopping...\r\n");
233     memset(lastState, '\0',BUF_SIZE);
```

```
234     strcpy(lastState,"stop.");
235   }
236   else if(strcmp(buf->Buffer,"battery.") == 0)
237   {
238     batCheck();
239     sprintf(TX_SEND, "%s %s %s", "Battery status: ", batStat, "V\r\n");
240     /*if(normFlg == 1)
241     {
242       sprintf(TX_SEND, "%s %s %s", "Battery status: ", batStat, "V\r\n")
      ;
243     }
244     else if(normFlg == -1)
245     {
246       strcpy(TX_SEND,"Warning: Battery Low...\r\n");
247     }*/
248     normFlg = 0, repFlg = 1;
249   }
250   else
251   {
252     strcpy(TX_SEND,"Invalid command...\r\n");
253   }
254   memset(buf->Buffer, '\0', BUF_SIZE);
255   strcpy(buf->Buffer, TX_SEND);
256
257   readFlg = 0;
258   UDR0 = buf->Buffer[buf->index];   // Initiate transfer
259   UCSR0B |= (1<<TXEN0)|(1<<UDRIE0); // Enable transmission and UDR0
      empty interrupt
260 }
261 //-------------------------
262 // Map float function
263 //-------------------------
264 float mapFloat(int x, int in_min, int in_max, int out_min, int out_max)
```

```
{
  return (float)(x - in_min) * (out_max - out_min) / (in_max - in_min) +
    out_min;
}
//-------------------------
// Check battery status
//-------------------------
void batCheck()
{
  int bVolt = analogRead(A3); // Read the charge on the battery
  float bStat = mapFloat(bVolt, 0, 1023, 0, 5);
  bStat = bStat*4.2/5;

  memset(batStat, '\0', bat_buf); // Reset batStat
  dtostrf(bStat, 5,3, batStat);
  if(bStat < 3.8 && bStat > 3.6)
  {
    normFlg = -1;
  }
  else if(bStat <= 3.6)
  {
    digitalWrite(OFF_PIN, HIGH);  // Turn off power
  }
  else
  {
    memset(batStat, '\0', 5); // Reset batStat
    sprintf(batStat, "%.3f%", bStat);
    normFlg = 1;
  }
}
void Buffer_Init(u8buf *buf)
{
    buf->index = 0;     // Set index to start of buffer
```

```
297 }
298 void USART0_Init(void)
299 {
300     UBRR0H = (uint8_t)(UBRR_VALUE>>8);  // Set baud rate
301     UBRR0L = (uint8_t)UBRR_VALUE;
302     UCSR0C |= (1<<UCSZ01)|(1<<UCSZ00);  // Set frame format to 8 data
    bits, no parity, 1 stop bit
303     UCSR0B |= (1<<RXEN0) | (1<<RXCIE0); // Enable receive and RC
    complete interrupts
304 }
305 uint8_t Buffer_Write(u8buf *buf, uint8_t u8data)
306 {
307     if (buf->index<BUF_SIZE)
308     {
309         buf->Buffer[buf->index] = u8data; // Increment buffer index
310         buf->index++;
311         return 0;
312     }
313     else return 1;
314 }
315 // RX Complete interrupt service routine
316 ISR(USART_RX_vect)
317 {
318     uint8_t u8temp;
319     u8temp = UDR0;
320     // Check if period char or end of buffer
321     if ((Buffer_Write(&buf, u8temp) == 1)||(u8temp == '.'))
322     {
323         // Disable reception and RX Complete interrupt
324         UCSR0B &= ~((1<<RXEN0)|(1<<RXCIE0));
325         readFlg = 1;
326     }
327 }
```

```
328 uint8_t Buffer_Read(u8buf *buf, volatile uint8_t *u8data)
329 {
330     buf->index++;
331     UDR0 = buf->Buffer[buf->index];
332     if(buf->Buffer[buf->index] == '\n' || buf->index > BUF_SIZE)
333     {
334       return 1;
335     }
336     else return 0;
337 }
338 // UDR0 Empty interrupt service routine
339 ISR(USART_UDRE_vect)
340 {
341     // If index is not at start of buffer
342     if (Buffer_Read(&buf, &UDR0) == 1)
343     {
344         // Start over, Reset buffer
345         Buffer_Init(&buf);
346         flush_buf(&buf);
347         // Disable transmission and UDR0 empty interrupt
348         UCSR0B &= ~((1<<TXEN0)|(1<<UDRIE0));
349         // Enable reception and RC complete interrupt
350         UCSR0B |= (1<<RXEN0)|(1<<RXCIE0);
351     }
352 }
353 // Erase Buffer routine
354 void flush_buf(u8buf *buf)
355 {
356   memset(buf->Buffer, '\0', strlen(buf->Buffer));
357 }
358 // Delay function
359 void delayM(int t)
360 {
```

```
361   int Start_time = millis();
362   while((millis() - Start_time) < t)
363   {
364     // Wait for timer
365   }
366 }
```

## REFERENCES


[1] Alonzo Kelly et al. “Toward reliable off road autonomous vehicles operating in challenging environments”. In: *The International Journal of Robotics Research* 25.5-6 (2006), pp. 449–483.

[2] E Velenis, P Tsiotras, and J Lu. “Aggressive maneuvers on loose surfaces: Data analysis and input parametrization”. In: *2007 Mediterranean Conference on Control & Automation*. IEEE. 2007, pp. 1–6.

[3] Gordon F Hayhoe and PA Kopac. “Evaluation of winter-driving traction aids”. In: *NCHRP Research Results Digest* 133 (1982).

[4] Gerasimos Skouvaklis, Jane R Blackford, and Vasileios Koutsos. “Friction of rubber on ice: A new machine, influence of rubber properties and sliding parameters”. In: *Tribology International* 49 (2012), pp. 44–52.

[5] Brian Goldfain et al. “AutoRally: An Open Platform for Aggressive Autonomous Driving”. In: *IEEE Control Systems Magazine* 39.1 (2019), pp. 26–55.

[6] Grady Williams et al. “Aggressive driving with model predictive path integral control”. In: *2016 IEEE International Conference on Robotics and Automation (ICRA)*. IEEE. 2016, pp. 1433–1440.

[7] Paul Drews et al. “Aggressive deep driving: Model predictive control with a cnn cost model”. In: *arXiv preprint arXiv:1707.05303* (2017).

[8] George W Burkett, Steven A Velinsky, et al. *Evaluation of Devices for Improving Traction Control in Winter Conditions*. Tech. rep. California. Department of Transportation, 2016.

[9] Robert R Scheibe, Principal Mechanical Engineer, and Kenneth C Kirkland. *An overview of studded and studless tire traction and safety*. Tech. rep. Washington State Department of Transportation, 2002.

[10] Takeshi Aoki, Yuki Murayama, and Shigeo Hirose. “Development of a transformable three-wheeled lunar rover: Tri-Star IV”. In: *Journal of Field Robotics* 31.1 (2014), pp. 206–223.

[11] Ch Grand, Ph Bidaud, and N Jarrassé. “Innovative concept of unfoldable wheel with an active contact adaptation mechanism”. In: *12th IFToMM World Congress. Besancon*. Citeseer. 2007.

[12] Yoo-Seok Kim et al. “Wheel transformer: A miniaturized terrain adaptive robot with passively transformed wheels”. In: *2013 IEEE International Conference on Robotics and Automation*. IEEE. 2013, pp. 5625–5630.

[13] Jaejun Park, Do Hun Kong, and Hae-Won Park. “Design of Anti-Skid Foot With Passive Slip Detection Mechanism for Conditional Utilization of Heterogeneous Foot Pads”. In: *IEEE Robotics and Automation Letters* 4.2 (2019), pp. 1170–1177.

[14] Alan T Asbeck et al. “Climbing walls with microspines”. In: *IEEE ICRA*. Fla. 2006.

[15] Kalind Carpenter, Nick Wiltsie, and Aaron Parness. “Rotary microspine rough surface mobility”. In: *IEEE/ASME Transactions on Mechatronics* 21.5 (2015), pp. 2378–2390.

[16] Dae-Young Lee et al. “Origami wheel transformer: A variable-diameter wheel drive robot using an origami structure”. In: *Soft robotics* 4.2 (2017), pp. 163–180.

[17] Todd G Nelson et al. “Developable mechanisms on developable surfaces”. In: (2019).

[18] Keiji Nagatani, Mitsuhiro Kuze, and Kazuya Yoshida. “Development of transformable mobile robot with mechanism of variable wheel diameter”. In: *J. Robot. Mechatron* 19 (2007), pp. 252–253.

[19] Shigeo Hirose et al. “Design of terrain adaptive versatile crawler vehicle HELIOS-VI”. In: *Proceedings 2001 IEEE/RSJ International Conference on Intelligent Robots and Systems. Expanding the Societal Role of Robotics in the the Next Millennium (Cat. No. 01CH37180)*. Vol. 3. IEEE. 2001, pp. 1540–1545.

[20] Shen-Chiang Chen et al. “Quattroped: a leg–wheel transformable robot”. In: *IEEE/ASME Transactions On Mechatronics* 19.2 (2013), pp. 730–742.

[21] Yu She, Carter J Hurd, and Hai-Jun Su. “A transformable wheel robot with a passive leg”. In: *2015 IEEE/RSJ International Conference on Intelligent Robots and Systems (IROS)*. IEEE. 2015, pp. 4165–4170.

[22] Byron Spice. *Researchers Reinventing the Wheel for Vehicles of the Future - News - Carnegie Mellon University*. Oct. 2018.

[23] Zhiqing Li et al. “Design and basic experiments of a transformable wheel-track robot with self-adaptive mobile mechanism”. In: *2010 IEEE/RSJ International Conference on Intelligent Robots and Systems*. IEEE. 2010, pp. 1334–1339.

[24] Francois Michaud et al. “Multi-modal locomotion robotic platform using leg-track-wheel articulations”. In: *Autonomous Robots* 18.2 (2005), pp. 137–156.

[25] Christophe Grand et al. “Stability and traction optimization of a reconfigurable wheel-legged robot”. In: *The International Journal of Robotics Research* 23.10-11 (2004), pp. 1041–1058.

[26] Gen Endo and Shigeo Hirose. “Study on roller-walker (system integration and basic experiments)”. In: *Proceedings 1999 IEEE International Conference on Robotics and Automation (Cat. No. 99CH36288C)*. Vol. 3. IEEE. 1999, pp. 2032–2037.

[27] Johannes Gültlinger et al. “Investigations of road wear caused by studded tires”. In: *Tire Science and Technology* 42.1 (2014), pp. 2–15.

[28] James Ray Lundy et al. “Wheel track rutting due to studded tires”. In: *Transportation Research Record* (1992), pp. 18–18.

[29] John Lindbom et al. “Exposure to wear particles generated from studded tires and pavement induces inflammatory cytokine release from human macrophages”. In: *Chemical research in toxicology* 19.4 (2006), pp. 521–530.

[30] Andy Watts et al. “The technology and economics of in-wheel motors”. In: *SAE International Journal of Passenger Cars-Electronic and Electrical Systems* 3.2010-01-2307 (2010), pp. 37–55.

[31] Juan De Santiago et al. “Electrical motor drivelines in commercial all-electric vehicles: A review”. In: *IEEE Transactions on vehicular technology* 61.2 (2011), pp. 475–484.

[32] Gen Endo and Shigeo Hirose. “Study on roller-walker-energy efficiency of roller-walk”. In: *2011 IEEE International Conference on Robotics and Automation*. IEEE. 2011, pp. 5050–5055.

[33] Thomas Hiller, Arnar Steingrimsson, and Robert Melvin. “Expanding the small auv mission envelope; longer, deeper & more accurate”. In: *2012 IEEE/OES Autonomous Underwater Vehicles (AUV)*. IEEE. 2012, pp. 1–4.

[34] Thomas Franke et al. “Experiencing range in an electric vehicle: Understanding psychological barriers”. In: *Applied Psychology* 61.3 (2012), pp. 368–391.

[35] Shigeo Hirose, Kan Yoneda, and Hideyuki Tsukagoshi. “TITAN VII: Quadruped walking and manipulating robot on a steep slope”. In: *Proceedings of International Conference on Robotics and Automation*. Vol. 1. IEEE. 1997, pp. 494–500.

[36] Yasuhiro Fukuoka et al. “Adaptive dynamic walking of a quadruped robot’Tekken’on irregular terrain using a neural system model”. In: *2003 IEEE International Conference on Robotics and Automation (Cat. No. 03CH37422)*. Vol. 2. IEEE. 2003, pp. 2037–2042.

[37] Alexander S Boxerbaum et al. “The latest generation whegs™ robot features a passive-compliant body joint”. In: *2008 IEEE/RSJ International Conference on Intelligent Robots and Systems*. IEEE. 2008, pp. 1636–1641.

[38] Abigail Klein Leichman. *Traction invention conquers ice, snow, sand, mud*. Jan. 2013.

[39] Rudolph R Hegmon. *Tire-pavement interaction*. Tech. rep. SAE Technical Paper, 1987.

[40] BE Lindenmuth. “An overview of tire technology”. In: *The pneumatic tire* (2005), p. 1.

[41] Joost J Kalker. *Three-dimensional elastic bodies in rolling contact*. Vol. 2. Springer Science & Business Media, 2013.

[42] A Arvanitaki et al. “The friction and lubrication of elastomers”. In: *Tribology Series*. Vol. 30. Elsevier, 1995, pp. 503–511.

[43] Gert Heinrich. “Hysteresis friction of sliding rubbers on rough and fractal surfaces”. In: *Rubber chemistry and technology* 70.1 (1997), pp. 1–14.

[44] Desmond F. Moore. *The friction and lubrication of elastomers, by Desmond F. Moore*. [1st ed.] Pergamon Press Oxford, New York, 1972, xvii, 288 p. ISBN: 0080167497.

[45] Avraham Harnoy, Bernard Friedland, and Simon Cohn. “Modeling and measuring friction effects”. In: *IEEE Control Systems Magazine* 28.6 (2008), pp. 82–91.

[46] David A Haessig Jr and Bernard Friedland. “On the modeling and simulation of friction”. In: (1991).

[47] V Van Geffen. *A study of friction models and friction compensation*. 2009.

[48] Sam Ella et al. “Investigation of rubber friction on snow for tyres”. In: *Tribology International* 59 (2013), pp. 292–301.

[49] Noriyuki Fukuoka. “Advanced technology of the studless snow tire”. In: *JSAE review* 15.1 (1994), pp. 59–66.

[50] Hamid Taghavifar and Aref Mardani. “Off-road vehicle dynamics”. In: *Studies in Systems, Decision and Control* 70 (2017), p. 37.

[51] Raymond Nen Yong, Ezzat A Fattah, and Nicolas Skiadas. *Vehicle traction mechanics*. Elsevier, 2012.

[52] Alan G Veith. “Tire Traction vs. Tread Compound Properties—How Pavement Texture and Test Conditions Influence the Relationship”. In: *Rubber chemistry and technology* 69.4 (1996), pp. 654–673.

[53] Bo NJ Persson et al. “Rubber friction on wet and dry road surfaces: The sealing effect”. In: *Physical review B* 71.3 (2005), p. 035428.

[54] RSH Richardson and H Nolle. “Surface friction under time-dependent loads”. In: *Wear* 37.1 (1976), pp. 87–101.

[55] JAC Martins, JT Oden, and FMF Simoes. “A study of static and kinetic friction”. In: *International Journal of Engineering Science* 28.1 (1990), pp. 29–92.